



Synthesis and structural characterization of ruthenium(II) and iron(II) complexes containing 1,2-di-(2-thienyl)-ethene derived ligands as chromophores

M. Helena Garcia^{a,*}, Pedro Florindo^a, M. Fátima M. Piedade^b, M. Teresa Duarte^b, M. Paula Robalo^{b,c}, Etienne Goovaerts^d, Wim Wenseleers^d

^a Centro de Ciências Moleculares e Materiais, Faculdade de Ciências da Universidade de Lisboa, Ed. C8, Campo Grande, 1749-016 Lisboa, Portugal

^b Centro de Química Estrutural, Instituto Superior Técnico, Universidade Técnica de Lisboa, Av. Rovisco Pais, 1049-001 Lisboa, Portugal

^c Departamento de Engenharia Química, Instituto Superior de Engenharia de Lisboa, Rua Conselheiro Emídio Navarro, 1, 1959-007 Lisboa, Portugal

^d Physics Department, University of Antwerp (UIA), Universiteitsplein 1, 2610 Wilrijk-Antwerpen, Belgium

ARTICLE INFO

Article history:

Received 23 July 2008

Received in revised form 6 November 2008

Accepted 7 November 2008

Available online 14 November 2008

Keywords:

Ruthenium(II)

Iron(II)

Monocyclopentadienyl

1,2-Di-(2-thienyl)-ethene nitrile ligands

Cyclic voltammetry

Nonlinear optics

ABSTRACT

A new family of three-legged piano stool structured organometallic compounds containing the η^5 -cyclopentadienylruthenium(II)/iron(II) fragments $\{M(\eta^5\text{-C}_5\text{H}_5)(\text{DPPE})\}^+$, $\{\text{Ru}(\eta^5\text{-C}_5\text{H}_5)(\text{PPh}_3)_2\}^+$ and $\{\text{Ru}(\eta^5\text{-C}_5\text{H}_5)(\text{TMEDA})\}^+$ with coordinated thiophene based chromophores, namely 5-(2-thiophen-2-yl-vinyl)-thiophene-2-carbonitrile (L1) and 5-[2-(5-Nitro-thiophen-2-yl)-vinyl]-thiophene-2-carbonitrile (L2) has been synthesized and fully characterized by ^1H , ^{13}C , ^{31}P NMR, IR and UV–Vis spectroscopies. Also, electrochemical studies were carried out by cyclic voltammetry and all experimental data are interpreted and compared with related compounds under the scope of NLO properties. Compounds $[\text{Ru}(\eta^5\text{-C}_5\text{H}_5)(\text{DPPE})(\text{NC}(\text{C}_4\text{H}_2\text{S})\text{C}(\text{H})\text{C}(\text{H})(\text{C}_4\text{H}_2\text{S}))][\text{CF}_3\text{SO}_3]$ (1^{Ru}) $[\text{Fe}(\eta^5\text{-C}_5\text{H}_5)(\text{DPPE})(\text{NC}(\text{C}_4\text{H}_2\text{S})\text{C}(\text{H})\text{C}(\text{H})(\text{C}_4\text{H}_2\text{S}))][\text{PF}_6]$ (1^{Fe}) and $[\text{Ru}(\eta^5\text{-C}_5\text{H}_5)(\text{DPPE})(\text{NC}(\text{C}_4\text{H}_2\text{S})\text{C}(\text{H})\text{C}(\text{H})(\text{C}_4\text{H}_2\text{S})\text{NO}_2)][\text{CF}_3\text{SO}_3]$ (4^{Ru}) were also crystallographically characterized.

© 2008 Elsevier B.V. All rights reserved.

1. Introduction

Since the report by Green et al. [1], revealing good second harmonic generation efficiencies for ferrocenyl derivatives, the interest in organometallic chemistry for the development of new NLO materials has increased considerably, motivated by the potential relevance of these materials in optical device technology [2–9]. In order to obtain a nonzero second-order response (molecular hyperpolarizability β), strongly asymmetric systems are needed. These systems can be obtained by combining a π -conjugated chain with electron donor and/or acceptor groups (D- π -A or push–pull systems) in which metal centers can behave either as acceptor or donor group by simply varying the metal and/or its oxidation state. Although interesting results have been achieved with ferrocene systems [10], half-sandwich complexes, in which the metal center is coplanar with the π -conjugated backbone, have boosted the NLO response of organometallic complexes. Concerning this feature, systematic studies were made on η^5 -monocyclopentadienylmetal complexes with benzene-based conjugated ligands bound to the metal center through nitrile or acetylide linkages [11–15]. Iron and ruthenium organometallic moieties have proven to be very efficient donor groups for second-order NLO purposes,

leading to higher β values than the usual organic groups (NR_2 , NH_2 , etc.).

Thiophene moiety has been studied as chromophore both in organic [16–18] and organometallic [19–25] materials for NLO and it is nowadays recognized to exhibit enhanced second-order polarizabilities compared to π -systems with phenylene bridges, mainly due to its lower delocalization energy, leading to a more effective conjugation. We recently reported the synthesis and NLO properties of η^5 -monocyclopentadienyliron(II) complexes with substituted oligo-thiophene nitrile derived ligands [26]. The observed constancy of β_0 upon chain-lengthening was attributed to a lowering of the charge transfer efficiency with increasing conjugation length, considering torsion angles in oligo-thiophenes to be small and thus not a significant factor to be considered in the observed trend [27,28]. In order to complement this study and also to confirm these conclusions, a set of new compounds was synthesized, where the extension of the π system was featured by the introduction of one vinylene unit between two thiophene rings, also assuring the planarity of the chromophore.

The new compounds of general formula $[\text{M}(\eta^5\text{-C}_5\text{H}_5)(\text{LL})(\text{NC}(\text{C}_4\text{H}_2\text{S})\text{C}(\text{H})\text{C}(\text{H})(\text{C}_4\text{H}_2\text{S})\text{Z})][\text{Y}]$, with $\text{Z} = \text{H}$, NO_2 ($\text{M} = \text{Ru}$, $\text{LL} = \text{DPPE}$ $\{\text{Y} = \text{PF}_6^-, \text{CF}_3\text{SO}_3^-\}$, 2PPh_3 $\{\text{Y} = \text{PF}_6^-\}$, TMEDA $\{\text{Y} = \text{PF}_6^-\}$; $\text{M} = \text{Fe}$, $\text{LL} = \text{DPPE}$ $\{\text{Y} = \text{PF}_6^-\}$) were characterized by the usual FT-IR, UV–Vis, ^1H , ^{13}C and ^{31}P NMR spectroscopic techniques. The organometallic fragment $[\text{Ru}(\eta^5\text{-C}_5\text{H}_5)(\text{TMEDA})]^+$ was introduced

* Corresponding author.

E-mail addresses: lena.garcia@ist.utl.pt, lena.garcia@fc.ul.pt (M.H. Garcia).

in these studies to evaluate the effect of the amine coligand on the donor ability of the organometallic moiety, relatively to the $[\text{Ru}(\eta^5\text{-C}_5\text{H}_5)(\text{PP})]^+$ fragment (PP = DPPE and PPh_3) currently used in our published studies [8,11–13]. The electrochemical studies were performed by means of cyclic voltammetry in order to get an insight on the electronic properties of the complexes and the results, together with the spectroscopic data, are discussed under the scope of the structural features that can be related to the NLO properties. X-ray diffraction studies of compounds $[\text{Ru}(\eta^5\text{-C}_5\text{H}_5)(\text{DPPE})(\text{NC}(\text{C}_4\text{H}_2\text{S})\text{C}(\text{H})\text{C}(\text{H})(\text{C}_4\text{H}_3\text{S}))][\text{CF}_3\text{SO}_3]$ (**1Ru**) $[\text{Fe}(\eta^5\text{-C}_5\text{H}_5)(\text{DPPE})(\text{NC}(\text{C}_4\text{H}_2\text{S})\text{C}(\text{H})\text{C}(\text{H})(\text{C}_4\text{H}_3\text{S}))][\text{PF}_6]$ (**1Fe**) and $[\text{Ru}(\eta^5\text{-C}_5\text{H}_5)(\text{DPPE})(\text{NC}(\text{C}_4\text{H}_2\text{S})\text{C}(\text{H})\text{C}(\text{H})(\text{C}_4\text{H}_2\text{S})\text{NO}_2)]\text{-}[\text{CF}_3\text{SO}_3]$ (**4Ru**) are also discussed.

2. Results and discussion

2.1. Synthesis of the ligands

The thiophene chromophores 5-(2-thiophen-2-yl-vinyl)-thiophene-2-carbonitrile (**L1**) and 5-[2-(5-nitro-thiophen-2-yl)-vinyl]-thiophene-2-carbonitrile (**L2**) were synthesized according to general procedures. The parent molecule 1,2-di-(2-thienyl)-ethene (**1**) was prepared with good yield from 2-thiophenecarboxaldehyde, by McMurry reaction [29]. Formylation of the thiophene unit was achieved by treatment of **1** with DMF and phosphorous oxychloride (Vilsmeier–Haack reaction). Reaction

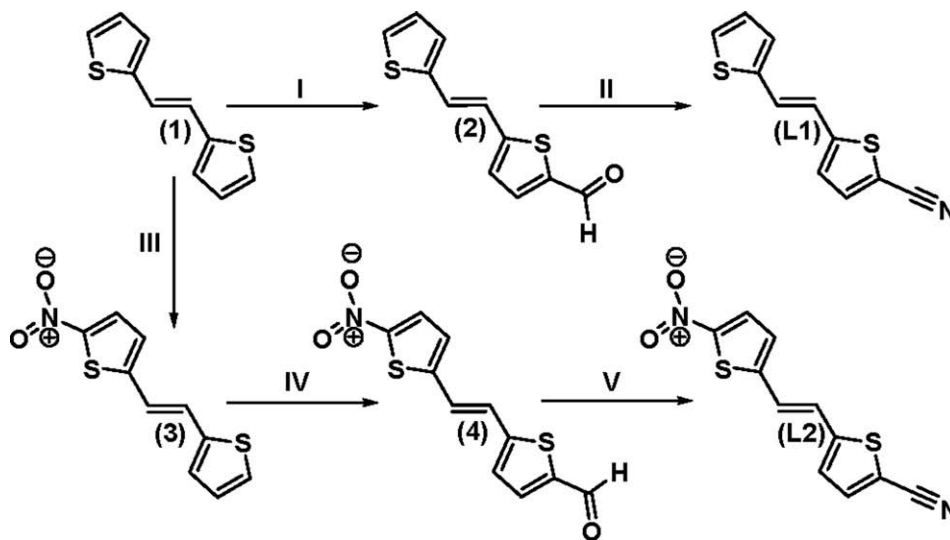
of the aldehyde **2** with hydroxylammonium chloride in pyridine and dehydration with acetic anhydride led to **L1**. Reaction of **1** with nitric acid in acetic acid afforded 2-nitro-5-(2-thiophen-2-yl-vinyl)-thiophene (**3**); **L2** was then obtained from **3**, by formylation and reduction to nitrile, applying the procedure described above for the synthesis of **L1**. All these reactions are summarized in Scheme 1.

The new nitrile ligands, obtained with yields of 74% (**L1**) and 33% (**L2**) from **1**, were fully characterized by IR, ^1H and ^{13}C NMR spectroscopies. Elemental analyses are in accordance with the proposed formulations.

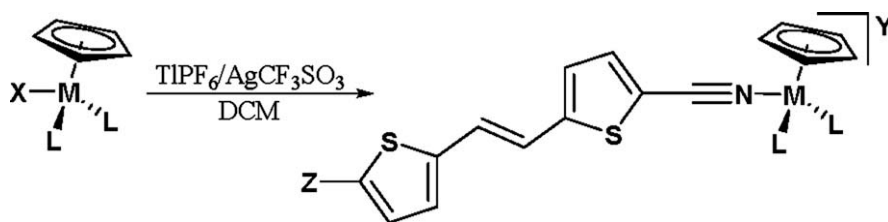
The solid state FT-IR spectra (KBr pellets) showed the characteristic stretching vibration of the nitrile functional group at $\approx 2215\text{ cm}^{-1}$ for both compounds. The FT-IR spectrum of **L2** also shows the NO_2 stretching bands at 1483 and 1337 cm^{-1} .

2.2. Synthesis of the Ru(II)/Fe(II) complexes

Complexes of general formula $[\text{M}(\eta^5\text{-C}_5\text{H}_5)(\text{LL})(\text{NC}(\text{C}_4\text{H}_2\text{S})\text{C}(\text{H})\text{C}(\text{H})(\text{C}_4\text{H}_2\text{S})\text{Z})][\text{Y}]$, with Z = H, NO_2 ; M = Ru, LL = DPPE {Y = PF_6^- , CF_3SO_3^- , 2PPh_3 {Y = PF_6^- }, TMEDA {Y = PF_6^- }; M = Fe, LL = DPPE {Y = PF_6^- }, were prepared by halide abstraction with a salt of the adequate counter-ion, in dichloromethane, from the corresponding neutral complex $[\text{M}(\eta^5\text{-C}_5\text{H}_5)(\text{LL})\text{X}]$ (M = Fe(II), X = I; M = Ru(II), X = Cl), in the presence of a slight excess of the corresponding nitrile (Scheme 2).



Scheme 1. Synthesis of nitrile ligands 5-(2-thiophen-2-yl-vinyl)-thiophene-2-carbonitrile (**L1**) and 5-[2-(5-nitro-thiophen-2-yl)-vinyl]-thiophene-2-carbonitrile (**L2**). (I) DMF, POCl_3 ; (II) (i) $\text{H}_2\text{NOH}\cdot\text{HCl}$, (ii) Ac_2O ; (III) HNO_3 , AcOH ; (IV) DMF, POCl_3 ; (V) (i) $\text{H}_2\text{NOH}\cdot\text{HCl}$, (ii) Ac_2O .



Scheme 2. Synthesis of the new complexes $[\text{M}(\eta^5\text{-C}_5\text{H}_5)(\text{LL})(\text{NC}(\text{C}_4\text{H}_2\text{S})\text{C}(\text{H})\text{C}(\text{H})(\text{C}_4\text{H}_2\text{S})\text{Z})][\text{Y}]$.

- 1Ru** M = Ru; (LL) = DPPE; Z = H; Y = PF₆⁻
1'Ru M = Ru; (LL) = DPPE; Z = H; Y = CF₃SO₃⁻
1Fe M = Fe; (LL) = DPPE; Z = H; Y = PF₆⁻
2Ru M = Ru; (LL) = TMEDA; Z = H; Y = PF₆⁻
3Ru M = Ru; (LL) = 2PPh₃; Z = H; Y = PF₆⁻
4Ru M = Ru; (LL) = DPPE; Z = NO₂; Y = PF₆⁻
4'Ru M = Ru; (LL) = DPPE; Z = NO₂; Y = CF₃SO₃⁻
4Fe M = Fe; (LL) = DPPE; Z = NO₂; Y = PF₆⁻
5Ru M = Ru; (LL) = TMEDA; Z = NO₂; Y = PF₆⁻
6Ru M = Ru; (LL) = 2PPh₃; Z = NO₂; Y = PF₆⁻

Reactions were carried out at room temperature, stirring overnight, under inert atmosphere. Compounds were recrystallized from dichloromethane/*n*-hexane, *n*-heptane or diethyl ether, affording crystalline yellow or orange products. With exception of compounds **2Ru** and **5Ru**, which revealed to be very sensitive to air, all compounds were fairly stable to air and moisture, either in the solid state or in solution and were obtained in good yields of 70–90%. The formulation is supported by FT-IR and ¹H, ¹³C, ³¹P NMR spectroscopic data and by elemental analysis.

The solid state IR spectra of the complexes present the characteristic bands of the cyclopentadienyl ligand (≈3050 cm⁻¹), the PF₆⁻ (840 and 560 cm⁻¹) or CF₃SO₃⁻ anions (1250 cm⁻¹) and the coordinated nitrile (2193–2214 cm⁻¹). As observed before for other related η⁵-monocyclopentadienyliron/ruthenium compounds, negative shifts, in the range –3 to –21 cm⁻¹, were observed on ν_{NC} by comparison with the corresponding values of the uncoordinated nitrile. This effect has been attributed to π-backdonation, due to π bonding between the d orbitals of the metal and the π* orbital of the nitrile group, which leads to a decrease in N≡C bond order [30]; accordingly, the highest negative shift of –21 cm⁻¹ was found for the iron derivative **4Fe**, which presents the good NO₂ acceptor group in the ligand structure. Surprisingly, compounds presenting TMEDA as coligand, instead of phosphines, showed even higher negative shifts on ν_{NC}, although no other evidence of π-backdonation has been found in the remaining spectroscopic studies. This effect might be due to the proximity of the TMEDA coligand due to the shorter distance Ru–N when compared to Ru–P in the equivalent compounds with DPPE or PPh₃ coligands, and was also observed for other ruthenium complexes with nitrogen ligands, where the effect of backdonation was not noticed [31].

¹H NMR resonances for the cyclopentadienyl ring are in the characteristic range of monocationic ruthenium(II) and iron(II) complexes. The effect of coordination on the nitrile ligands is observed through the shielding of the first thiophene ring protons, especially for the H₃ protons (see Fig. 1 for numbering scheme), indicating an electronic flow towards the aromatic ligand due to π-backdonation involving the metal centre. This effect is very pronounced in the complexes with DPPE, showing the better σ-donor ability of this coligand, with shieldings on H₃ up to 1.2 ppm, upon coordination. In the complexes involving the **L1** ligand, the shielding effect is noticed only on H₃, H₄ and H₆, but in the complexes with **L2** all the aromatic protons show a significant shielding (see Table 1), this indicating that the electronic flow is extended

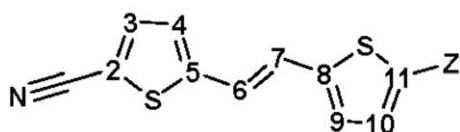


Fig. 1. Numbering scheme for NMR spectral assignments of Ru/Fe complexes and free ligands.

Table 1

Selected ¹H NMR data for ligands **L1** and **L2**, free and coordinated to Ru/Fe organometallic fragments.

Compound	Proton							η-C ₅ H ₅
	H3	H4	H6	H7	H9	H10	H11	
L1	d 7.75	d 7.31	d 7.44	d 7.21	d 7.32	m 7.09	d 7.49	–
1Ru	d 6.76	d 7.28	d 7.30	d 7.07	d 7.09	m 7.10	d 7.51	s 5.04
1'Ru	d 6.77	d 7.27	d 7.32	d 7.05	d 7.10	m 7.14	d 7.49	s 5.02
1Fe	d 6.72	d 7.04	d 7.04	d 7.24	d 7.27	m 7.08	d 7.48	s 4.67
2Ru	br 7.93	d 7.38	d 7.47	d 7.24	d 7.31	m 7.11	d 7.52	s 4.32
3Ru	d 7.52	^a	^a	d 7.20	d 7.31	m 7.11	^a	s 4.76
L2	d 7.96	d 7.51	d 7.53	d 7.69	d 7.44	d 8.12	–	–
4Ru	d 6.82	d 7.24	d 7.32	d 7.48	d 7.36	d 7.99	–	s 5.03
4'Ru	d 6.82	d 7.20	d 7.33	d 7.47	d 7.36	d 8.00	–	s 5.02
4Fe	d 6.79	d 7.21	d 7.29	d 7.46	d 7.36	d 7.99	–	s 4.70
5Ru	br 7.99	d 7.53	d 7.50	d 7.64	d 7.40	d 8.01	–	s 4.34
6Ru	d 7.58	–	–	d 7.60	d 7.58	d 8.00	–	s 4.77

^a Masked by phosphine protons signals.

throughout the entire π-system, due to the pull effect of the NO₂ group.

In the complexes with TMEDA coligand, this shielding effect is not observed, despite the negative shift on ν_{NC} found for these the complexes, marginally higher than for the corresponding DPPE complexes. It also worth mentioning that for compounds with TMEDA as coligand, namely **2Ru** and **5Ru**, the Cp ring is shielded, relatively to the compounds with phosphines as coligands, in both ¹H and ¹³C NMR spectra. These facts seem to indicate that the electron density is trapped in the metal centre and that π-backdonation effect is limited only to the nitrile group, without delocalization along the chromophore.

¹³C NMR data shows that the carbons of the chromophore ligands remained almost unchanged or suffered a slight deshielding upon coordination, except for the carbon of the nitrile group which is clearly deshielded due to σ coordination to the metal centre.

³¹P{¹H} NMR data of the complexes showed a single sharp signal for the phosphine coligands (DPPE and PPh₃) revealing the equivalency of the two phosphorus atoms, and an expected deshielding upon coordination, in accordance with its σ donor character.

2.3. UV-Visible studies

The optical absorption spectra of all the synthesized new complexes were recorded in ~5 × 10⁻⁵ mol dm⁻³ solutions of dichloromethane and methanol (Table 2) in order to identify any metal-to-ligand charge transfer band (MLCT) and the π–π* absorption bands, expected for these complexes.

In order to understand the effect of the substituting groups on the **L1** and **L2** chromophores, the electronic spectra of 1,2-di-(2-thienyl)-ethene (**1**) and 2-nitro-5-(2-thiophen-2-yl-vinyl)-thiophene (**3**) were also obtained. These electronic spectra are shown together in Fig. 2, for comparison.

As expected, the introduction of the acceptor group NO₂ leads to a bathochromic shift of the π–π* transition band, while the nitrile group leads only to changes in band intensity, in relation to compound **1**. The electronic spectrum of **L2** is similar to the one of **3**, presenting a slightly more energetic π–π* transition band (20 nm).

The electronic spectra of all the complexes (see Fig. 3) showed two intense absorption bands in the UV region, attributed to electronic transitions occurring in the organometallic fragment [MCp(LL)]⁺ (λ ≈ 240 nm) and coordinated chromophores

Table 2

Optical spectra data for Ru(II)/Fe(II) complexes and organic compounds **1**, **3**, **L1** and **L2** in CH₂Cl₂ and MeOH (ca. 5 × 10⁻⁵ M) solutions.

Compound	λ_{max} (nm) (ϵ , M ⁻¹ cm ⁻¹)	
	CH ₂ Cl ₂	MeOH
1,2-di-(2-thienyl)-ethene (1)	260(6000)	
	342(21 800)	
2-Nitro-5-(2-thiophen-2-yl-vinyl)-thiophene (3)	286(11 200)	
	421(19 300)	
5-(2-Thiophen-2-yl-vinyl)-thiophene-2-carbonitrile (L1)	258(12 400)	
	341(10 000)	
[Ru(η^5 -C ₅ H ₅)(DPPE)(L1)][PF ₆] (1Ru)	382(23 500)	383(24 000)
[Ru(η^5 -C ₅ H ₅)(DPPE)(L1)][CF ₃ SO ₃] (1' Ru)	383(23 100)	385(24 100)
[Fe(η^5 -C ₅ H ₅)(DPPE)(L1)][PF ₆] (1Fe)	411(28 200)	407(28 800)
[Ru(η^5 -C ₅ H ₅)(TMEDA)(L1)][PF ₆] (2Ru)	271(12 400)	272(11 900)
	385(28 200)	391(26 600)
[Ru(η^5 -C ₅ H ₅)(PPh ₃) ₂ (L1)][PF ₆] (3Ru)	391(28 200)	388(27 500)
5-[2-(5-Nitro-thiophen-2-yl)-vinyl]-thiophene-2-carbonitrile (L2)	290(11 000)	
	401(20 000)	
[Ru(η^5 -C ₅ H ₅)(DPPE)(L2)][PF ₆] (4Ru)	422(26 900)	419(21 700)
[Ru(η^5 -C ₅ H ₅)(DPPE)(L2)][CF ₃ SO ₃] (4' Ru)	421(27 200)	417(22 600)
[Fe(η^5 -C ₅ H ₅)(DPPE)(L2)][PF ₆] (4Fe)	406(20 500)	400(25 300)
[Ru(η^5 -C ₅ H ₅)(TMEDA)(L2)][PF ₆] (5Ru)	292(12 500)	305(9800)
	405(28 200)	417(24 000)
[Ru(η^5 -C ₅ H ₅)(PPh ₃) ₂ (L2)][PF ₆] (6Ru)	425(26 800)	433(25 400)

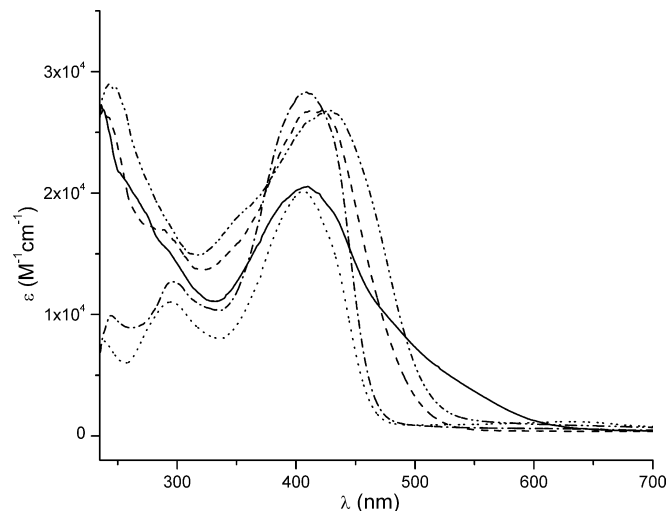


Fig. 3. Electronic spectra for complexes **4Ru** (---), **4Fe** (—), **5Ru** (— · —), **6Ru** (····) and the uncoordinated ligand **L2** (····) in dichloromethane.

2.4. Electrochemical studies

In order to get an insight on the electron richness of the organometallic fragment and the coordinated chromophores, the electrochemical behavior of Ru(II) and Fe(II) compounds and the free ligands, **L1** and **L2**, was studied by cyclic voltammetry in dichloromethane and acetonitrile, between the limits imposed by the solvents. Compounds possessing TMEDA as coligand, **2Ru** and **5Ru**, were not studied due to fast decomposition in our current experi-

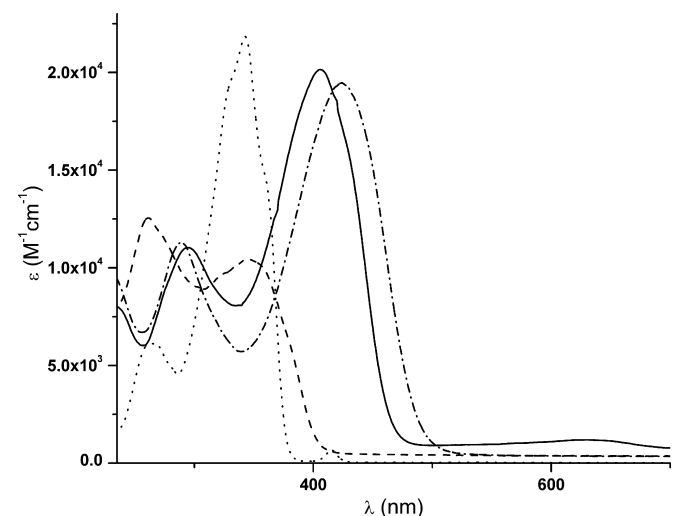


Fig. 2. Electronic spectra of compounds **1** (····), **3** (— · —), **L1** (---) and **L2** (—), recorded in $\sim 5 \times 10^{-5}$ mol dm⁻³ dichloromethane solutions.

($\lambda \approx 380$ – 425 nm). No other defined bands can be observed. Nonetheless, the broadening of the π - π^* absorption bands in the spectra, particularly for **1Fe** and **4Fe**, indicating a complex structure, let us suspect that a new MLCT band might be overlapped with these bands. Our previous results for η^5 -monocyclopentadienyliron(II) complexes with substituted oligo-thiophene nitrile ligands [26], showed that chain-lengthening leads to a bathochromic shift of the π - π^* transitions and to a hypsochromic shift of the MLCT band. Since complexes [M(η^5 -C₅H₅)(LL)(NC(C₄H₂S)C(H)C(H)(C₄H₂S)Z)][Y] have approximately the same conjugation length of the complexes [FeCp(P-P)(NC(C₄H₂S)₃NO₂)] [PF₆], for which the referred overlap was observed, the present assumptions seem therefore quite pertinent.

No visible solvatochromic effect was verified for the complexes due to the small polarity difference between dichloromethane and methanol, although shifts may be masked by the intense π - π^* absorption bands.

Table 3

Electrochemical data for complexes [M(η^5 -C₅H₅)(LL)(NC(C₄H₂S)C(H)C(H)(C₄H₂S)Z)][PF₆] and for organic compounds **1**, **3**, **L1** and **L2**, in dichloromethane.

Compound	E_{pa} (V)	E_{pc} (V)	$E_{\text{p1/2}}$ (V)	$E_{\text{pa}} - E_{\text{pc}}$ (mV)	$I_{\text{a}}/I_{\text{c}}$
1,2-di-(2-thienyl)-ethene (1)	1.28	—	—	—	—
	—	0.36 ^a	—	—	—
2-Nitro-5-(2-thiophen-2-yl-vinyl)-thiophene (3)	1.58	—	—	—	—
	-0.83	-1.01	—	—	—
5-(2-Thiophen-2-yl-vinyl)-thiophene-2-carbonitrile (L1)	1.51	—	—	—	—
[Ru(η^5 -C ₅ H ₅)(DPPE)(L1)][PF ₆] (1Ru)	1.51	—	—	—	—
	1.28	1.12	—	—	—
	—	-1.50	—	—	—
[Fe(η^5 -C ₅ H ₅)(DPPE)(L1)][PF ₆] (1Fe)	1.54	—	—	—	—
	0.88	0.77	0.83	110	≈ 1
	—	-1.46	—	—	—
[Ru(η^5 -C ₅ H ₅)(PPh ₃) ₂ (L1)][PF ₆] (3Ru)	1.43	1.30 ^b	—	—	—
	1.32	1.11 ^b	—	—	—
	—	-1.49	—	—	—
5-[2-(5-Nitro-thiophen-2-yl)-vinyl]-thiophene-2-carbonitrile (L2)	1.23	—	—	—	—
	-0.74	-0.98	—	—	—
	-1.15	-1.36	—	—	—
[Ru(η^5 -C ₅ H ₅)(DPPE)(L2)][PF ₆] (4Ru)	1.27	1.15	1.21	110	—
	-0.73	-0.88	—	—	—
	-1.04	-1.18	—	—	—
[Fe(η^5 -C ₅ H ₅)(DPPE)(L2)][PF ₆] (4Fe)	0.88	0.78	0.83	100	≈ 1
	-0.71	-0.86	—	—	—
	-1.03	-1.18	—	—	—
[Ru(η^5 -C ₅ H ₅)(PPh ₃) ₂ (L2)][PF ₆] (6Ru)	1.41	—	—	—	—
	1.23	—	—	—	—
	-0.77	-0.92	—	—	—
	-1.00 ^b	-1.12	—	—	—
	-1.15 ^b	-1.28	—	—	—

^a Attributed to a decomposition product originated by the irreversible oxidation.

^b Extremely weak.

Table 4

Electrochemical data for complexes $[M(\eta^5\text{-C}_5\text{H}_5)(\text{LL})(\text{NC}(\text{C}_4\text{H}_2\text{S})\text{C}(\text{H})\text{C}(\text{H})(\text{C}_4\text{H}_2\text{S})\text{Z})][\text{PF}_6]$ and for the organic compounds **1**, **3**, **L1** and **L2** in acetonitrile.

Compound	E_{pa} (V)	E_{pc} (V)	$E_{\text{p}1/2}$ (V)	$E_{\text{pa}}-E_{\text{pc}}$ (mV)	$I_{\text{a}}/I_{\text{c}}$
1,2-di-(2-thienyl)-ethene (1)	1.12	–	–	–	–
2-Nitro-5-(2-thiophen-2-yl-vinyl)-thiophene (3)	–1.04 1.44 –0.83 –1.53	–1.30	–	–	–
5-(2-Thiophen-2-yl-vinyl)-thiophene-2-carbonitrile (L1)	1.42	–	–	–	–
	–	–0.12 ^a –0.85 ^a	–	–	–
[Ru($\eta^5\text{-C}_5\text{H}_5$)(DPPE)(L1)][PF ₆] (1Ru)	–1.55 1.41 1.12	–1.70	–	–	–
	–	–1.53 ^b	–	–	–
[Fe($\eta^5\text{-C}_5\text{H}_5$)(DPPE)(L1)][PF ₆] (1Fe)	–1.60 1.41	–1.75	–	–	–
	0.77	0.62	0.69	150	≈1
	–	–1.46 ^b	–	–	–
	–	–1.73	–	–	–
[Ru($\eta^5\text{-C}_5\text{H}_5$)(PPh ₃) ₂ (L1)][PF ₆] (3Ru)	1.40 1.22	1.27 1.02	1.34	130	–
	–	–1.46 ^b	–	–	–
	–1.59	–1.71	–1.65	120	–
5-[2-(5-Nitro-thiophen-2-yl)-vinyl]-thiophene-2-carbonitrile (L2)	1.18	–	–	–	–
	–0.76	–0.91	–	–	–
	–1.16	–1.31	–	–	–
[Ru($\eta^5\text{-C}_5\text{H}_5$)(DPPE)(L2)][PF ₆] (4Ru)	1.13	0.98	–	–	–
	–0.74	–0.86	–0.80	120	–
	–1.04	–1.14	–1.09	100	–
	–1.16	–1.28	–1.22	120	–
[Fe($\eta^5\text{-C}_5\text{H}_5$)(DPPE)(L2)][PF ₆] (4Fe)	0.79	0.61	–	–	≈1
	–0.73	–0.86	–0.79	130	–
	–1.05	–1.17	–1.11	120	–
[Ru($\eta^5\text{-C}_5\text{H}_5$)(PPh ₃) ₂ (L2)][PF ₆] (6Ru)	1.23	1.03	–	–	–
	–0.73	–0.87	–	–	–
	–1.03	–1.13	1.08	100	–
	–1.18	–1.28	–1.23	100	–

^a Attributed to a decomposition product originated by the irreversible oxidation.

^b Extremely weak.

mental conditions. Compounds **1Ru** and **4Ru** were not studied, since the change of the counter-ion was not expected to influence the electrochemical behavior of the complexes, when compared with **1Ru** and **4Ru**, respectively. To complement our understanding about the effect of the substituting groups on the electrochemical behavior of the chromophores, the parent compound **1** and its nitro derivative **3** (see Scheme 1) were also studied. Relevant data for the redox changes exhibited by the studied compounds, in dichloromethane and acetonitrile, are summarized in Table 3 and Table 4, respectively.

The electrochemical behavior of organic compounds **1**, **3**, **L1** and **L2** is characterized by one irreversible oxidation, with E_{pa} ranging from 1.23 V to 1.58 V in dichloromethane and from 1.12 V to 1.44 V in acetonitrile, without any cathodic counterpart. Although this oxidation occurs at higher potentials for **3** and **L1** than for the parent compound **1**, due to the presence of the acceptor groups NO₂ and NC, respectively, **L2** does not follow the same trend, presenting only one weak oxidation wave at a potential very similar to **1**, (even lower in dichloromethane), suggesting the role of NC as a weak donor group in the presence of the good acceptor NO₂.

The cyclic voltammograms of the free ligand **L1** and the parent compound **1** (see Scheme 1) were quite similar in both solvents. In dichloromethane, the oxidation occurred at $E_{\text{pa}} = 1.51$ and 1.28 V, respectively, with no cathodic counterpart. After few sweeps, some additional oxidation and reduction broad waves were observed for both compounds, attributed to the product deposition observed at the platinum electrode surface, this being compatible with the expected potential-induced polymerization of thiophenes [32]. In

acetonitrile the oxidation processes occurred at lower potential as expected, namely $E_{\text{pa}} = 1.42$ V (**L1**) and $E_{\text{pa}} = 1.12$ V (compound **1**). The reduction of **L1** occurred at $E_{\text{pc}} = -1.70$ V ($E_{\text{pa}} = -1.55$ V) and compound **1** was reduced at $E_{\text{pc}} = -1.30$ V ($E_{\text{pa}} = -1.04$ V). In this solvent the polymerization process, leading to the deposition on the electrode surface, was only observed for compound **1**.

Compounds **3** and **L2**, were mostly characterized by two reductive irreversible processes in acetonitrile, due to the presence of the acceptor group NO₂, at $E_{\text{pc}}^1 = -0.95$ V ($E_{\text{pc}}^1 E_{\text{pa}}^2 = -0.83$ V) and $E_{\text{pc}}^2 = -1.67$ V ($E_{\text{pa}}^2 = -1.53$ V) for compound **3** while these processes became easier for **L2** due to the presence of the second acceptor group (N≡C–) $E_{\text{pc}}^1 = -0.91$ V ($E_{\text{pa}}^1 = -0.76$ V) and $E_{\text{pc}}^2 = -1.31$ V ($E_{\text{pa}}^2 = -1.16$ V). In dichloromethane only the second reductive process was found for compound **3**, $E_{\text{pc}}^2 = -1.01$ V ($E_{\text{pa}}^2 = -0.83$ V) although **L2** exhibits both processes in this solvent at $E_{\text{pc}}^1 = -0.98$ V ($E_{\text{pa}}^1 = -0.74$ V) and $E_{\text{pc}}^2 = -1.36$ V ($E_{\text{pa}}^2 = -1.15$ V).

The electrochemical behaviour of the iron complexes **1Fe** and **4Fe** in dichloromethane is characterized by an irreversible process at $E_{\text{p}1/2} = 0.83$ V and $E_{\text{pa}} = 0.88$ V for both complexes and attributed to the Fe(II)/Fe(III) redox pair. This seems to indicate that the presence of the NO₂ acceptor group in **4Fe** has little influence on the electron richness of the metal. It was also found that both compounds **L1** and **L2** are easier to reduce as coordinated ligands than as free compounds. The reduction process attributed to ligand **L1**, occurs in compound **1Fe** at $E_{\text{pc}} = -1.46$ V, while no reduction occurs for **L1** as free compound, within the limits imposed by dichloromethane. Similarly, the two reductive processes found for free compound **L2** at $E_{\text{pc}}^1 = -0.98$ V ($E_{\text{pa}}^1 = -0.74$ V) and $E_{\text{pc}}^2 = -1.36$ V ($E_{\text{pa}}^2 = -1.15$ V) became easier after coordination in compound **4Fe** where $E_{\text{pc}}^1 = -0.86$ V ($E_{\text{pa}}^1 = -0.71$ V) and $E_{\text{pc}}^2 = -1.18$ V ($E_{\text{pa}}^2 = -1.03$ V). Accordingly, it was found that the oxidation of **L1** and **L2** compounds was more difficult as coordinated ligands. Therefore, these observations all together indicate a regular dative sigma coordination of both ligands, without any effect of π backdonation as was suggested by our spectroscopic data.

The ruthenium(II) complexes show the same general behaviour of the iron ones, except for the higher potential of the Ru(II)/Ru(III) oxidation process, which being irreversible, present only very small cathodic counterpart. Again, the metal centres seem unaffected by the presence of the acceptor group in the coordinated chromophore, as observed by comparison of Ru(II)/Ru(III) oxidation potentials of **1Ru** and **3Ru** with the ones of **4Ru** and **6Ru**, respectively.

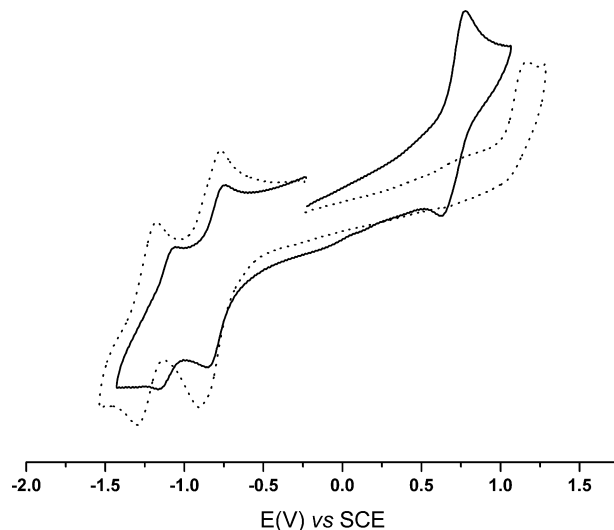


Fig. 4. Cyclic voltammograms of **4Fe** (—) and **L2** (···) ligand in acetonitrile.

On going to negative potentials, the electrochemical behaviour of the **L1** coordinated chromophore in the complexes **1Ru**, **1Fe** and **3Ru** shows the presence of one cathodic wave at -1.50 , -1.46 and -1.49 V in dichloromethane and -1.75 , -1.73 and -1.71 V in acetonitrile, showing that the coordination of **L1** either to Ru(II) or to Fe(II) leads to a more difficult reduction. Compounds with the **L2** coordinated chromophore **4Ru**, **4Fe** and **6Ru** present also the reductive processes occurring at a little lower potential than in the free ligand, due to the overall electron-withdrawing effect of the ligand. This effect is more pronounced in the second reduction potentials. The general electrochemical behaviour of these complexes is illustrated in Fig. 4, which shows the comparison of **4Fe** complex and the correspondent uncoordinated ligand **L2**.

The voltammograms of complexes $[\text{Ru}(\eta^5\text{-C}_5\text{H}_5)(\text{DPPE})(\text{L2})][\text{PF}_6]$ (**4Ru**) and $[\text{Ru}(\eta^5\text{-C}_5\text{H}_5)(\text{PPh}_3)_2(\text{L2})][\text{PF}_6]$ (**6Ru**) in acetonitrile revealed one additional third wave at $E_{\text{pa}} \sim -1.04$ and $E_{\text{pc}} \sim -1.14$ V which origin can possibly be explained by the formation of a new product originated by substitution of the coordinated phosphine, since this process was more evident in the case of the compound with PPh_3 as coligands. Also, the wave relative to the oxidation $\text{Ru}^{\text{II}}/\text{Ru}^{\text{III}}$ showed some asymmetry compatible with two oxidative processes. No further studies were carried out to confirm this hypothesis, since the compounds are stable in the solvents of interest for NLO measurements, namely dichloromethane and chloroform.

In view of the comparison of the compounds studied in this work to other related metallothiophene derivatives for which some studies of second-order nonlinear optics were performed [26], it is of interest to evaluate the HOMO–LUMO gap, expressed by the difference between the first oxidation and reduction potentials. As assumed before [26], the M(II)/M(III) oxidation and the first reduction potential can be related, respectively, to the relative magnitude of the HOMO and the LUMO energies. This assumption considers that the HOMO is essentially located in the metal fragment and the LUMO in the nitrile ligand, as showed by the Extended Hückel MO calculations performed in other similar complexes containing *p*-benzonitrile derivatives [12]. In the present work the HOMO–LUMO gap was estimated for compounds **4Ru** and **4Fe** and the results are presented in Table 5, together with the values already reported for other related thiophene derivatives [26,33].

The data show that the HOMO–LUMO gap depends on the metal fragment and the solvent used in the electrochemical experiments. The HOMO–LUMO gap is higher for the ruthenium complex **4Ru** than for the iron derivative **4Fe**, with differences of 0.41 V and 0.37 V in dichloromethane and acetonitrile, respectively. This is mainly due to the stabilization of the HOMO orbital for the ruthenium complex, since the LUMO is almost unaffected by the change

of metal fragment. These results are in agreement with the better donor character of the iron(II) fragment.

The HOMO–LUMO gaps estimated for compounds **4Ru** and **4Fe** (Table 5) are similar to the values found for $[\text{M}(\eta^5\text{-C}_5\text{H}_5)(\text{DPPE})(\text{NC}\{\text{C}_4\text{H}_2\text{S}\}_3\text{NO}_2)][\text{PF}_6]$ complexes, **C'** and **C**, in agreement with the similar conjugation length of the chromophores. For both complexes, the lower HOMO–LUMO gaps obtained in acetonitrile are mainly due to the relative stabilization of the HOMO orbital in this solvent, since the first reduction potential (LUMO), related to the thiophene coordinated ligand, remain almost unchanged. This is in disagreement with the large LUMO stabilizations verified for compounds $[\text{MCp}(\text{DPPE})(\text{NC}\{\text{C}_4\text{H}_2\text{S}\}_n\text{NO}_2)][\text{PF}_6]$ ($n = 2, 3$), specially for the iron compounds, for which LUMO stabilizations of 90 mV (**B**) and 100 mV (**C**) are verified, and this might be related to conformational changes in oligo-thiophene ligand structures due to different solvent polarity, thus leading to a significant energy lowering effect on LUMO. Ab initio calculations, suggesting that terthiophene geometry are very sensitive to the chemical environment [27], and the fact that no LUMO stabilization is verified for compound **4Fe**, further supports this assumption. Although the same trend is verified for the ruthenium analogues, LUMO stabilizations are lower, which may be attributed to the weaker donor character of the $[\text{RuCp}(\text{DPPE})]^+$ moiety in relation to $[\text{FeCp}(\text{DPPE})]^+$, leading to a lower push effect.

The HOMO–LUMO gap can also be correlated with the solvatochromic behaviour in the electronic spectra of the complexes, indicative of a bathochromic shift of the MLCT with increasing solvent polarity, which is characteristic of electronic transitions with an increase of the dipole moment upon photo-excitation. However, in the present case, solvatochromic behaviour of the MLCT band could not be clearly identified due to overlapping of this transition with the one attributed to the coordinated thiophene ligand.

Also, it might be of interest the comparison of the M(II)/M(III) oxidation potentials of compounds **4Fe** and **4Ru** to the oxidation potentials of the related sets of iron(II) (**A**, **B** and **C**) and ruthenium(II) (**A'**, **B'** and **C'**) derivatives in which the oligo-thiophene chromophores present 2, 4 and 6 double bonds, as presented in Table 5. Although the increase in conjugation length leads to a decrease in M(II)/M(III) oxidation potential within the series of compounds $[\text{M}(\eta^5\text{-C}_5\text{H}_5)(\text{DPPE})(\text{NC}\{\text{C}_4\text{H}_2\text{S}\}_n\text{NO}_2)][\text{PF}_6]$ [26,33], compounds **4Ru** and **4Fe** do not follow this trend, showing higher oxidation potentials, in both solvents, than compounds **B'** and **B**, respectively, despite the increase in conjugation length. This is clearly illustrated in Fig. 5, which presents the variation of the M(II)/M(III) oxidation potentials with the number of double bonds of the chromophore, showing that the electronic density of the metal centre is less than expected attending only to chromophores conjugation length and suggesting improved metal–chromophore conjugation for compounds **4Fe** and **4Ru**.

Table 5

Estimation of HOMO–LUMO gap based on electrochemical data for selected compounds.

Compound	E_{ox} (V)		E_{red} (V)		HOMO–LUMO (V)	
	CH_2Cl_2	CH_3CN	CH_2Cl_2	CH_3CN	CH_2Cl_2	CH_3CN
$[\text{FeCp}(\text{dppe})(\text{L2})][\text{PF}_6]$ (4Fe)	0.88	0.79	−0.86	−0.86	1.74	1.65
$[\text{FeCp}(\text{dppe})(\text{NC}\{\text{C}_4\text{H}_2\text{S}\}\text{NO}_2)][\text{PF}_6]^{\text{a}}$ A	0.91	0.83	−0.66	−0.64	1.57	1.47
$[\text{FeCp}(\text{dppe})(\text{NC}\{\text{C}_4\text{H}_2\text{S}\}_2\text{NO}_2)][\text{PF}_6]^{\text{a}}$ B	0.85	0.76	−0.86	−0.77	1.71	1.55
$[\text{FeCp}(\text{dppe})(\text{NC}\{\text{C}_4\text{H}_2\text{S}\}_3\text{NO}_2)][\text{PF}_6]^{\text{a}}$ C	0.81	0.75	−0.94	−0.84	1.75	1.59
$[\text{RuCp}(\text{dppe})(\text{L2})][\text{PF}_6]$ (4Ru)	1.27	1.13	−0.88	−0.86	2.15	1.99
$[\text{RuCp}(\text{dppe})(\text{NC}\{\text{C}_4\text{H}_2\text{S}\}\text{NO}_2)][\text{PF}_6]^{\text{b}}$ A'	1.33	1.16	−0.65	−0.62	1.98	1.78
$[\text{RuCp}(\text{dppe})(\text{NC}\{\text{C}_4\text{H}_2\text{S}\}_2\text{NO}_2)][\text{PF}_6]^{\text{b}}$ B'	1.23	1.12	−0.82	−0.79	2.05	1.91
$[\text{RuCp}(\text{dppe})(\text{NC}\{\text{C}_4\text{H}_2\text{S}\}_3\text{NO}_2)][\text{PF}_6]^{\text{b}}$ C'	1.22	1.11	−0.91	−0.87	2.13	1.98

^a Ref. [26].

^b Ref. [33].

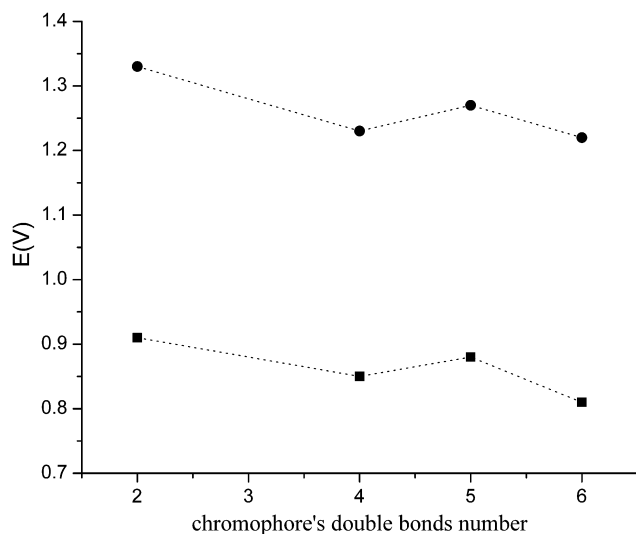


Fig. 5. Variation of Ru^{II}/Ru^{III} (●) and Fe^{II}/Fe^{III} (■) oxidation potentials with the number of chromophore double bonds of compounds [M(η⁵-C₅H₅)(DPPE)(NC(C₄H₂S)_nNO₂)]⁺[PF₆]⁻ [26,33] and 4Ru/4Fe, in dichloromethane.

Table 6

Selected bond lengths [Å] and bond and torsion angles [°].

Bond lengths	1Ru	4Ru	1Fe
M–Cp ^a	1.8575(3)	1.8593(5)	1.7061(12)
M–N(1)	2.016(3)	1.997(5)	1.865(8)
N(1)–C(1)	1.151(5)	1.148(8)	1.164(11)
C(1)–C(2)	1.414(5)	1.436(10)	1.404(13)
C(2)–S(1)	1.736(4)	1.700(8)	1.717(9)
C(2)–C(3)	1.376(6)	1.368(11)	1.347(12)
C(3)–C(4)	1.409(6)	1.398(11)	1.374(13)
C(4)–C(5)	1.377(7)	1.323(12)	1.363(12)
C(5)–S(1)	1.733(4)	1.715(8)	1.721(8)
C(5)–C(6)	1.453(6)	1.426(11)	1.438(12)
C(6)–C(7)	1.343(7)	1.295(14)	1.327(13)
C(7)–C(8)	1.456(6)	1.464(14)	1.438(13)
C(8)–S(2)	1.719(5)	1.702(12)	1.715(9)
C(8)–C(9)	1.367(7)	1.300(17)	1.337(13)
C(9)–C(100)	1.421(8)	1.303(17)	1.409(15)
C(100)–C(101)	1.326(10)	1.41(2)	1.319(15)
C(101)–S(2)	1.710(8)	1.685(12)	1.701(11)
M(1)–P(1)	2.2834(10)	2.2803(16)	2.210(3)
M(1)–P(2)	2.2913(11)	2.2724(17)	2.201(3)
Angles			
N(1)–M(1)–P(1)	86.38(9)	89.12(16)	86.5(2)
N(1)–M(1)–P(2)	92.67(10)	89.84(16)	91.6(2)
P(2)–M(1)–P(1)	84.17(4)	84.35(6)	86.95(10)
Cp ^a –M(1)–N(1)	125.43(7)	126.55(14)	124.0(2)
Cp ^a –M(1)–P(1)	129.66(2)	128.93(5)	130.15(9)
Cp ^a –M(1)–P(2)	125.56(2)	126.91(5)	125.17(8)
M(1)–N(1)–C(1)	178.2(3)	175.8(5)	175.4(7)
N(1)–C(1)–C(2)	177.8(4)	176.4(7)	176.3(10)
Torsion angles			
M(1)–N(1)–C(1)–C(2)	75(18)	–7(21)	39(23)
N(1)–C(1)–C(2)–C(3)	122(13)	93(14)	–90(15)
N(1)–C(1)–C(2)–S(1)	–55(13)	–82(14)	88(15)
C(1)–C(2)–C(3)–C(4)	–177.4(4)	–174.3(7)	177.2(9)
C(5)–C(6)–C(7)–C(8)	173.0(4)	179.0(8)	–178.0(9)

^a Cp centroid.

2.5. X-ray structural studies

X-ray diffraction studies were performed on single crystals of the new compounds [Ru(η⁵-C₅H₅)(DPPE)(NC(C₄H₂S)C(H)C(H)(C₄H₃S))]–[PF₆]⁻ (**1Ru**) [Fe(η⁵-C₅H₅)(DPPE)(NC(C₄H₂S)C(H)C(H)(C₄H₃S))]–[PF₆]⁻ (**1Fe**) and [Ru(η⁵-C₅H₅)(DPPE)(NC(C₄H₂S)C(H)C(H)(C₄H₂S)NO₂)]–

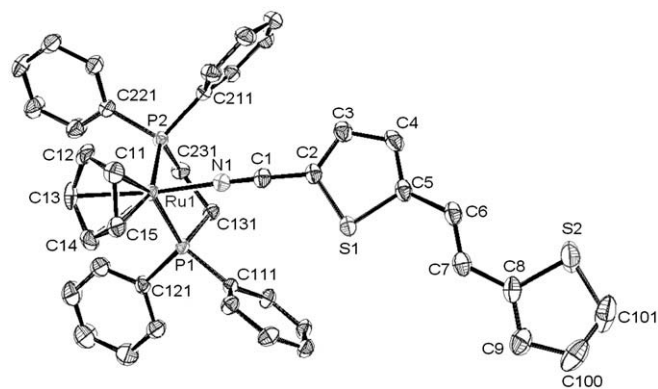


Fig. 6. Molecular diagram of cation **1Ru** showing the numbered atoms.

[PF₆]⁻ (**4Ru**), obtained by slow diffusion of *n*-hexane in dichloromethane solutions of compounds **1Ru** and **1Fe** and *n*-hexane/acetone for **4Ru**. Compounds **1Fe**, and **4Ru** crystallized in the monoclinic spatial groups *C2/c* and *P2₁/n*, respectively and compound **1Ru** in the orthorhombic *Pbca* spatial group. Selected bond distances and bond and torsion angles for these three compounds are presented in Table 6, and molecular schemes and numbering are depicted in Figs. 6–8.

All the complexes present a distorted three-legged piano stool geometry around the metal atom, confirmed by the P–M–P and (C≡N)–M–P angles close to 90°, with the remaining C(η⁵-centroid)–M–N(≡C) and C(η⁵-centroid)–M–P angles between 124.0° and 130.15°. The dihedral angles between the planes of the thiophene rings in compounds **1Fe** (7.06°) and **4Ru** (8.39°) are clearly lower than the corresponding ones in the related compounds [RuCp(DPPE)(NC(C₄H₂S)₂NO₂)]⁺[PF₆]⁻ (17.6°) [33] and [RuCp(DPPE)(NC(C₆H₄)₂NO₂)]⁺[PF₆]⁻ (14.47°) [34]. This observation is in agreement with the chromophore's planarity improvement predicted for the present compounds and suggests that dihedral angle between thiophene rings may in fact have some influence in the loss of charge transfer efficiency with increasing conjugated length suggested for compounds [FeCp(DPPE)(NC(C₄H₂S)_nNO₂)]⁺[PF₆]⁻ (*n* = 2, 3) [26]. For compound **1Ru** the dihedral angle is 17.64°, clearly superior to the ones found for **1Fe** and **4Ru**, which might be explained by inferior conjugation along the chromophore in **1Ru** due to the combination of the organometallic donor [RuCp(DPPE)]⁺, a worst donor in relation to the iron analogue in **1Fe**, and **1L**, in which the acceptor group is absent in relation to **4Ru**.

All the Ru compounds show bond distances Ru–N as well the N–C placed in the range of the ones found for similar cyclopentadienyldiphosphine complexes with thiophene based nitrile ligands (Ru–N 1.977–2.023 Å and N–C 1.139–1.178 Å) but smaller, in general, than the ones found in cyclopentadienyldiphosphine complexes with NCPH ligands presented on Table 7. Despite the fact that some results, such as for example Ru–N distances, might suggest some evidence for π backdonation for the present compounds, compared to other related nitriles, a careful study of the other coordination geometrical parameters do not led us to any conclusion or evidence about the significance of this effect.

For **1Fe**, although NC bond distance (1.164(11) Å) is somewhat higher than for compound **1Ru** (1.151(5) Å), and C1–C2 distance somewhat shorter (1.404(13) Å versus 1.414(5) Å for **1Ru**) suggesting some evidence for π-backdonation supported also by the spectroscopic data, no conclusions can be drawn due to the large error associated to **1Fe** bond distances.

The bond angles M–N≡C of the studied compounds present only a slight deviation of the linearity, with values in accordance to the ones found for related compounds (see Table 7).

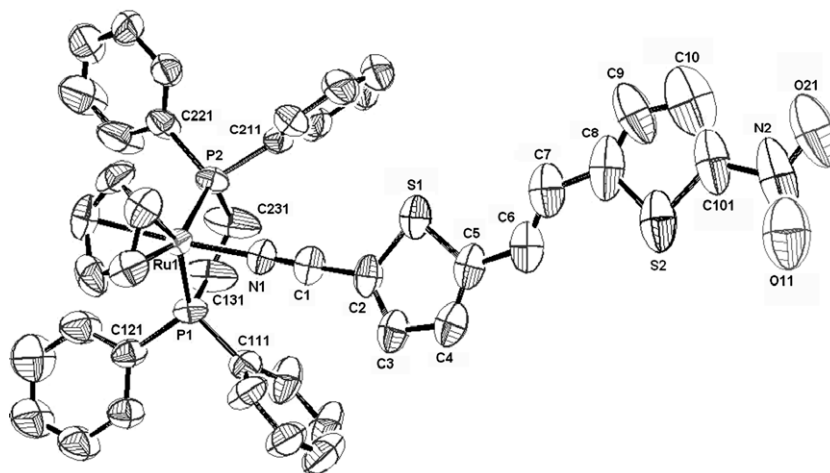


Fig. 7. Molecular diagram of cation **4Ru**, showing the numbered atoms.

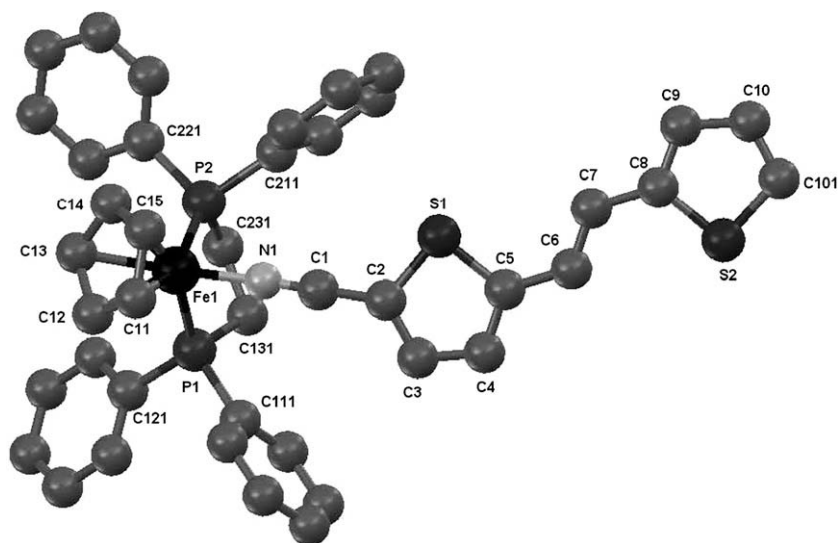


Fig. 8. Molecular diagram of cation **1Fe**, showing the numbered atoms, done with MERCURY. The ellipsoids are not shown due to severe anisotropy in some atoms.

Table 7
Selected geometrical parameters for ruthenium and iron derivatives containing CpM(phosphine)nitrile cations and the ones presented in this work.

Compound	M–N (Å)	N–C (Å)	C–C (Å)	M–N–C (°)	N–C–C (°)
[RuCp(DPPE)(L1)][CF ₃ SO ₃] (1Ru)	1.8575(3)	1.151(5)	1.414(5)	178.2(3)	177.8(4)
[RuCp(DPPE)(L2)][CF ₃ SO ₃] (4Ru)	1.997(5)	1.148(8)	1.436(10)	175.8(5)	176.4(7)
[RuCp(PPh ₃) ₂ (NCPH)][PF ₆] ^a	2.037(1)	1.145(2)	1.440(2)	171.70(12)	177.84(16)
[RuCp(PPh ₃) ₂ (NCPHNO ₂)][PF ₆] ^a	2.023(2)	1.146(2)	1.442(3)	171.24(15)	177.8(2)
[RuCp(PPh ₃) ₂ (NCPHMe ₂)][PF ₆] ^a	2.031(1)	1.149(2)	1.424(2)	173.52(14)	175.15(18)
[RuCp(DPPE)(NCPH ₂ NO ₂)][PF ₆] ^b	2.030(3)	1.136(5)	1.441(6)	177.4(3)	177.7(4)
[RuCp(PPh ₃) ₂ (NC{BDT})][PF ₆] ^c	1.995(6)	1.117(10)	1.464(12)	176.6(7)	176.0(9)
[RuCp(PPh ₃) ₂ (NC{BDT})][CF ₃ SO ₃] ^c	2.025(5) 2.016(6)	1.153(8), 1.151(9)	1.402(9), 1.416(10)	176.3(5) 169.8(6)	173.4(7), 178.6(7)
[RuCp(DPPE)(NC{BDT})][PF ₆] ^c	2.018(4)	1.149(6)	1.400(7)	176.7(4)	176.3(6)
[RuCp(DPPE)(NC(C ₄ H ₂ S) ₂ NO ₂)][PF ₆] ^d	2.002(5)	1.144(6)	1.411(7)	175.4(5)	177.1(7)
[FeCp(DPPE)(L1)][CF ₃ SO ₃] (1Fe)	1.865(8)	1.164(11)	1.404(13)	175.4(7)	176.3(10)
[FeCp(DPPE)(NCPH)][PF ₆] ^a	1.892(2)	1.141(3)	1.444(3)	172.16(18)	174.5(2)
[FeCp(DPPE)(NCC ₆ H ₄ NO ₂)][PF ₆] ^e	1.874(11)	1.129(14)	1.42(2)	176.6(11)	177.4(15)
[FeCp(DPPE)(NCPHNO ₂)] ^f	1.875(13)	1.390(19)	1.40(2)	175.6(11)	178.0(16)
[FeCp(PROPHOS)(NCPHNO ₂)][PF ₆] ^g	1.902(9)	1.12(15)	1.421(15)	172.0(10)	172.8(13)
[FeCp(DPPE)(NC{BDT})][PF ₆] ^c	1.8639(4)	1.154(6)	1.427(8)	176.6(4)	178.1(5)

BDT = benzo[1,2-b;4,3-b']dithiophene; PROPHOS- (R)-(-)-1,2-bis(diphenylphosphino)propane.

^a Ref. [35].

^b Ref. [34].

^c Ref. [31].

^d Ref. [33].

^e Ref. [12].

^f Ref. [36].

^g Ref. [37].

Table 8
Details of data collection and structure refinement for compound **1Ru**.

Compound	1Ru	4Ru	1Fe
Chemical formula	C ₄₃ H ₃₆ F ₃ NO ₃ P ₂ RuS ₃	C ₄₃ H ₃₅ F ₃ N ₂ O ₅ P ₂ RuS ₃	C ₄₂ H ₃₆ F ₆ FeNS ₂ P ₃
Molecular weight	930.92	975.92	881.60
T (K)	150(2)	150(2)	293(2)
Wavelength	0.71069	0.71069	0.71069
Crystal system	Orthorhombic	Monoclinic	Monoclinic
Space group	<i>Pbca</i>	<i>P2(1)/n</i>	<i>C2/c</i>
<i>a</i> (Å)	17.2060(17)	10.7230(5)	26.486(3)
<i>b</i> (Å)	20.266(2)	8.5910(4)	23.188(2)
<i>c</i> (Å)	23.493(3)	50.918(2)	16.616(2)
β (°)	–	95.734(3)	125.828(10)
<i>V</i> (Å ³)	8191.9(16)	4667.2(4)	8273.9(17)
<i>Z</i>	8	4	8
<i>D</i> _{calc} (g cm ⁻³)	1.510	1.389	1.415
Absorption coefficient (mm ⁻¹)	0.668	0.594	0.640
<i>F</i> (000)	3792	1984	3616
θ Range for data collection (°)	1.78–30.68	2.86–25.37	2.59–25.35
Limiting indices	–24 ≤ <i>h</i> ≤ 14; –26 ≤ <i>k</i> ≤ 29; –33 ≤ <i>l</i> ≤ 33	–12 ≤ <i>h</i> ≤ 11; –10 ≤ <i>k</i> ≤ 10; –60 ≤ <i>l</i> ≤ 61	–31 ≤ <i>h</i> ≤ 25; –27 ≤ <i>k</i> ≤ 0; 0 ≤ <i>l</i> ≤ 20
Reflections collected/unique	74122/12617 [<i>R</i> _{int} = 0.0661]	58030/8483 [<i>R</i> _{int} = 0.0502]	7828/7549 [<i>R</i> _{int} = 0.0770]
Completeness to θ	30.68 (99.4%)	25.37 (99.0%)	25.35 (99.9%)
Refinement method	Full-matrix least-squares on <i>F</i> ²		
Data/restraints/parameters	12617/0/513	8483/0/540	7549/350/510
Goodness-of-fit on <i>F</i> ²	1.021	1.115	1.001
Final <i>R</i> indices [<i>I</i> > 2 σ (<i>I</i>)]	<i>R</i> ₁ = 0.0454; <i>wR</i> ₂ = 0.1030	<i>R</i> ₁ = 0.0764; <i>wR</i> ₂ = 0.1874	<i>R</i> ₁ = 0.0899; <i>wR</i> ₂ = 0.1879
Largest difference in peak/hole (e Å ⁻³)	1.207/–1.014	1.046/–1.318	0.616/–0.521

Detailed analysis of the geometric parameters in the three compounds, led us to notice that in compounds **1Ru**, **4Ru** and **1Fe**, the plane of the thiophene ring closest to the metal centre is almost perpendicular in relation to the plane defined by the metal atom, the centroid of the cyclopentadienyl and the N1 and C1 atoms making a dihedral angle of 76.99(6)° and 80.66(27)° 82.83(19)°, respectively. As discussed before [31], the referred angle seems to depend on the interplay of energetic stability and stereochemical hindrance, with parameters such as the cone angle and mono or bidentate behaviour of the coordinated phosphine, size of the chromophore and supramolecular interactions in the crystal packing, playing an important role.

3. Conclusions

A new family of Ru(II) and Fe(II) three-legged piano stool complexes was synthesised and fully characterized. Spectroscopic and electrochemical data show that 1,2-di-(2-thienyl)-ethene moiety allows an improved electron-donor effect from the metal centre towards NO₂ acceptor group. Also, electrochemical and crystallographic data show improved planarity of the chromophore, allowing a superior conjugation between the metal centre and the acceptor group, despite the increase in conjugation length. Thus, we are expecting improved NLO properties for these compounds, compared with our related published compounds possessing oligo-thiophene nitrile derived ligands. Studies of the molecular hyperpolarizability β by Hyper Rayleigh Scattering (HRS) for this new family of compounds are currently in progress.

4. Experimental

4.1. General procedures

All the experiments were carried out under dinitrogen atmosphere using standard Schlenk techniques. All solvents were dried using standard methods [38]. Starting materials were prepared

following the methods described in the literature: [Ru(η^5 -C₅H₅)(DPPE)Cl] and [Ru(η^5 -C₅H₅)(PPh₃)₂Cl] [39], [Fe(η^5 -C₅H₅)(DPPE)I] [12], [Ru(η^5 -C₅H₅)(TMEDA)Cl] [40], 1,2-di-(2-thienyl)-ethene [29]. Solid state IR spectra were taken on a Mattson Satellite FTIR spectrophotometer with KBr pellets; only significant bands are cited in the text. ¹H, ¹³C and ³¹P NMR spectra were recorded on a Bruker Avance 400 spectrometer at probe temperature. The ¹H and ¹³C chemical shifts are reported in parts per million (ppm) downfield from internal Me₄Si and the ³¹P NMR spectra are reported in ppm downfield from external standard H₃PO₄ 85%. Coupling constants are reported in Hz. Spectral assignments of the organic ligands follow the numbering scheme shown in Fig. 1.

Electronic spectra were recorded at room temperature on a Jasco V-560 spectrometer in the range of 200–900 nm. Microanalyses were performed using a Fisons Instruments EA1108 system. Data acquisition, integration and handling were performed using a PC with the software package Eager-200 (Carbo Erba Instruments).

4.2. Synthesis of the ligands

4.2.1. 5-(2-Thiophen-2-yl-vinyl)-thiophene-2-carbaldehyde (**2**)

1,2-Di-(2-thienyl)-ethene (1.9 g, 10 mmol) was dissolved in 1,2-dichloroethane (20 mL) and DMF (1.1 mL, 12 mmol). The solution was cooled to 5 °C and POCl₃ (1.5 mL, 12 mmol) was added dropwise. The mixture was then heated to reflux for 4 h. After cooling, 50 mL of saturated solution of NaCO₂CH₃ were added and the mixture was stirred for a further hour. The mixture was then extracted with dichloromethane, washed with a saturated solution of NaHCO₃, water and dried over magnesium sulphate. The solvent was removed under vacuum and the product was purified by flash column chromatography (eluent: light petroleum/dichloromethane 6:4) to give 1.8 g (82%) of the desired product as yellow needles. IR (KBr, cm⁻¹): ν (C=O) 1655 cm⁻¹. ¹H NMR (Acetone-*d*₆): 7.01(m, 1H, H₁₀), 7.21(d, 1H, H₇, ³*J*_{HH} = 16.0 Hz), 7.31(d, 1H, H₉, ³*J*_{HH} = 3.4 Hz), 7.36(d, 1H, H₄, ³*J*_{HH} = 3.9 Hz), 7.48(d, 1H, H₆, ³*J*_{HH} = 16.0 Hz), 7.49(d, 1H, H₁₁, ³*J*_{HH} = 5.2 Hz), 7.88(d, 1H, H₃, ³*J*_{HH} = 3.9 Hz), 9.91(s, 1H, CHO). ¹³C NMR (Acetone-*d*₆): 120.20(C₂), 125.63(C₆), 126.49(C₁₁),

127.19(C₄), 128.09(C₁₀), 128.45(C₉), 137.94(C₃), 141.38(C₈), 141.79(C₅), 151.29(C₂), 182.69(CHO). Anal. Found: C, 59.92; H, 3.72%. Calc. for C₁₁H₈OS₂: C, 59.97; H, 3.66(%)

4.2.2. 5-(2-Thiophen-2-yl-vinyl)-thiophene-2-carbonitrile (**L1**)

A solution of H₂NOH · HCl (1.4 g, 20 mmol) in pyridine (4 mL) was added to a solution of 5-(2-thiophen-2-yl-vinyl)-thiophene-2-carbaldehyde (2.2 g, 10 mmol) in pyridine (20 mL), cooled to 5 °C. After stirring for 5 min at that temperature, acetic anhydride (10 mL) was added and the mixture was refluxed for 1 h. After cooling, the mixture was poured onto ice and the precipitate formed was filtered, washed with water, dissolved in dichloromethane and dried over magnesium sulphate. The solvent was removed under vacuum and the product was purified by flash column chromatography (eluent: light petroleum/dichloromethane 7:3) to give 1.9 g (90%) of the desired product as light yellow needles. IR (KBr, cm⁻¹): ν(N≡C) 2217. ¹H NMR (Acetone-*d*₆): 7.09(m, 1H, H₁₀), 7.21(d, 1H, H₇, ³J_{HH} = 16.0 Hz), 7.31(d, 1H, H₄, ³J_{HH} = 3.9 Hz), 7.32(d, 1H, H₉, ³J_{HH} = 3.4 Hz), 7.44(d, 1H, H₆, ³J_{HH} = 16.0 Hz), 7.49(d, 1H, H₁₁, ³J_{HH} = 5.1 Hz), 7.75(d, 1H, H₃, ³J_{HH} = 3.9 Hz). ¹³C NMR (Acetone-*d*₆): 106.48(C₂), 114.00(CN), 119.15(C₇), 125.54(C₆), 126.22(C₉), 126.48(C₁₁), 128.06(C₁₀), 128.46(C₄), 138.87(C₃), 141.15(C₈), 149.59(C₅). Anal. Found: C, 60.46; H, 3.37; N, 6.13%. Calc. for C₁₁H₇NS₂: C, 60.80; H, 3.25; N, 6.45(%)

4.2.3. 2-Nitro-5-(2-thiophen-2-yl-vinyl)-thiophene (**3**)

HNO₃ (0.70 mL, 10 mmol) was added to a solution of 1,2-di-(2-thienyl)-ethene (1.9 g, 10 mmol) in acetic acid (AcOH) (40 mL). After stirring for 2 h, the mixture was poured onto ice (100 mL). The precipitate was filtered, dissolved in dichloromethane, washed with a saturated solution of NaHCO₃ and water, dried with magnesium sulfate and pumped to dryness. The product was recrystallized from ethanol to give 1.2 g (51%) of the pure product as orange-red needles. IR (KBr, cm⁻¹): ν(NO₂) 1487 and 1320; δ(NO₂) 710; ¹H NMR (Acetone-*d*₆): 7.13(m, 1H, H₃), 7.21(d, 1H, H₆, ³J_{HH} = 16.0 Hz), 7.30(d, 1H, H₉, ³J_{HH} = 4.3 Hz), 7.37(d, 1H, H₄, ³J_{HH} = 3.4 Hz), 7.54(d, 1H, H₂, ³J_{HH} = 5.0 Hz), 7.60(d, 1H, H₆, ³J_{HH} = 16.0 Hz), 7.98(d, 1H, H₁₀, ³J_{HH} = 4.3 Hz). ¹³C NMR (Acetone-*d*₆): 119.39(C₆), 125.42(C₇), 126.82(C₂), 127.24(C₉), 128.20(C₃), 129.17(C₄), 130.20(C₁₀), 141.00(C₅), 148.91(C₈), 150.26(C₁₁). Anal. Found: C, 50.46; H, 2.78; N, 6.03%. Calc. for C₁₀H₇S₂NO₂: C, 50.62; H, 2.97; N, 5.90(%)

4.2.4. 5-[2-(5-Nitro-thiophen-2-yl)-vinyl]-thiophene-2-carbaldehyde (**4**)

2-Nitro-5-(2-thiophen-2-yl-vinyl)-thiophene (2.4 g, 10 mmol) was dissolved in 1,2-dichloroethane (20 mL) and DMF (1.1 mL, 12 mmol). The solution was cooled to 5 °C and POCl₃ (1.5 mL, 12 mmol) was added dropwise. The mixture was then heated to reflux for 24 h. After cooling, 50 mL of a saturated solution of NaCO₂CH₃ were added and the mixture was stirred for a further hour. The mixture was then extracted with dichloromethane, washed with saturated solution of NaHCO₃, water and dried over magnesium sulphate. The solvent was removed under vacuum and the product was purified by flash column chromatography (eluent: light petroleum/dichloromethane 1:1) to give 2.0 g (75%) of the desired product as yellow needles. IR (KBr, cm⁻¹): ν(C=O) 1658; ν(NO₂) 1484 and 1324; δ(NO₂) 730; ¹H NMR (DMSO-*d*₆): 7.43(d, 1H, H₄, ³J_{HH} = 3.9 Hz), 7.52(d, 1H, H₆, ³J_{HH} = 16.0 Hz), 7.53(d, 1H, H₄, ³J_{HH} = 4.3 Hz), 7.66(d, 1H, H₇, ³J_{HH} = 16.0 Hz), 7.96(d, 1H, H₃, ³J_{HH} = 3.9 Hz), 8.02(d, 1H, H₁₀, ³J_{HH} = 4.3 Hz), 9.97(s, 1H, CHO). ¹³C NMR (Acetone-*d*₆): 124.30(C₆), 126.36(C₇), 127.93(C₄), 130.23(C₉), 131.51(C₁₀), 139.19(C₃), 143.26(C₈), 143.35(C₅), 149.49(C₁₁), 149.74(C₂), 184.63(CHO). Anal. Found: C, 50.89; H, 2.33; N, 5.30%. Calc. for C₁₁H₇S₂NO₃: C, 49.80; H, 2.66; N, 5.28(%)

4.2.5. 5-[2-(5-Nitro-thiophen-2-yl)-vinyl]-thiophene-2-carbonitrile (**L2**)

A solution of H₂NOH · HCl (1.4 g, 20 mmol) in pyridine (4 mL) was added to a solution of 5-[2-(5-nitro-thiophen-2-yl)-vinyl]-thiophene-2-carbaldehyde (2.7 g, 10 mmol) in pyridine (20 mL), cooled to 5 °C. After stirring for 5 min at that temperature, acetic anhydride (10 mL) was added and the mixture was refluxed for 1 h. After cooling, the mixture was poured onto ice and the precipitate formed was filtered, washed with water, dissolved in dichloromethane and dried over magnesium sulphate. The solvent was removed under vacuum and the product was purified by flash column chromatography (eluent: light petroleum/dichloromethane 1:1) to give 2.3 g (86%) of the desired product as light yellow needles. IR (KBr, cm⁻¹): ν(CN) 2214; ν(NO₂) 1483 and 1337; δ(NO₂) 732; ¹H NMR (Acetone-*d*₆): 7.44(d, 1H, H₉, ³J_{HH} = 4.3 Hz), 7.51(d, 1H, H₄, ³J_{HH} = 3.2 Hz), 7.53(d, 1H, H₆, ³J_{HH} = 16.0 Hz), 7.69(d, 1H, H₇, ³J_{HH} = 16.0 Hz), 7.96(d, 1H, H₃, ³J_{HH} = 3.2 Hz), 8.12(d, 1H, H₁₀, ³J_{HH} = 4.3 Hz). Anal. Found: C, 50.31; H, 2.33; N, 10.41%. Calc. for C₁₁H₆S₂N₂O₂: C, 50.37; H, 2.31; N, 10.68(%)

4.3. Synthesis of the complexes

4.3.1. Preparation of [M(η⁵-C₅H₅)(LL)]

(NC(C₄H₂S)C(H)C(H)(C₄H₂S)Z)] [Y]

Complexes [M(η⁵-C₅H₅)(LL)(NCR)] [Y] were prepared by halide abstraction from the parent neutral complexes [M(η⁵-C₅H₅)(LL)X] (1 mmol) with TlPF₆ or AgCF₃SO₃ (1 mmol) in dichloromethane, in the presence of a slight excess of the ligand (1.1 mmol), at room temperature, for 16 h under inert atmosphere. After cooling to room temperature, filtering and removing the solvent, the complexes were washed with *n*-hexane (3 × 15 mL) and recrystallized from acetone or dichloromethane/*n*-heptane, *n*-hexane or diethyl ether giving crystalline products.

4.3.1.1. [Ru(η⁵-C₅H₅)(DPPE)(NC(C₄H₂S)C(H)C(H)(C₄H₂S))] [PF₆] (**1Ru**). Yellow; recrystallized from CH₂Cl₂/*n*-heptane); 75% yield; IR (KBr, cm⁻¹): ν(CN) 2212, ν_{as}(OSO, CF₃SO₃⁻) 1250; ¹H NMR (Acetone-*d*₆): 2.71(m, 2H, -CH₂-), 2.84(m, 2H, -CH₂-), 5.04(s, 5H, η⁵-C₅H₅), 6.76(d, 1H, H₃, ³J_{HH} = 4.0 Hz), 7.07(d, 1H, H₇, ³J_{HH} = 16.0 Hz), 7.09(d, 1H, H₉, ³J_{HH} = 4.0 Hz), 7.10(m, 1H, H₁₀), 7.28(d, 1H, H₄, ³J_{HH} = 4.0 Hz), 7.30(d, 1H, H₆, ³J_{HH} = 16.0 Hz), 7.51(d, 1H, H₁₁, ³J_{HH} = 4.8 Hz), 7.51(m, 10H, C₆H₅(DPPE)), 7.63(m, 6H, C₆H₅(DPPE)), 8.02(m, 4H, C₆H₅(DPPE)). ¹³C NMR (Acetone-*d*₆): 27.59(-CH₂-, DPPE), 82.57(η⁵-C₅H₅), 105.46(C₂), 118.63(C₇), 121.18(CN), 125.68(C₄), 125.92(C₆), 126.84(C₁₁), 128.01(C₁₀), 128.76(C₉), 129.05(CH, DPPE), 131.08(CH, DPPE), 133.26(CH, DPPE), 137.62(Cq, DPPE), 139.47(C₃), 140.93(C₈), 150.50(C₅). ³¹P NMR (Acetone-*d*₆): 79.1(s, DPPE). Anal. Found: C, 53.39; H, 4.14; N, 1.48%. Calc. for C₄₂H₃₆NS₂P₃F₆Ru · 0.3CH₂Cl₂: C, 53.35; H, 3.87; N, 1.47(%)

4.3.1.2. [Ru(η⁵-C₅H₅)(DPPE)(NC(C₄H₂S)C(H)C(H)(C₄H₂S))] [CF₃SO₃] (**1Ru**). Yellow; recrystallized from CH₂Cl₂/*n*-heptane); 75% yield; IR (KBr, cm⁻¹): ν(CN) 2212, ν_{as}(OSO, CF₃SO₃⁻) 1250; ¹H NMR (Acetone-*d*₆): 2.70(m, 2H, -CH₂-), 2.80(m, 2H, -CH₂-), 5.02(s, 5H, η⁵-C₅H₅), 6.77(d, 1H, H₃, ³J_{HH} = 4.0 Hz), 7.05(d, 1H, H₇, ³J_{HH} = 16.0 Hz), 7.10(d, 1H, H₉, ³J_{HH} = 4.0 Hz), 7.14(m, 1H, H₁₀), 7.27(d, 1H, H₄, ³J_{HH} = 4.0 Hz), 7.32(d, 1H, H₆, ³J_{HH} = 16.0 Hz), 7.49(d, 1H, H₁₁, ³J_{HH} = 4.8 Hz), 7.52(m, 10H, C₆H₅(DPPE)), 7.67(m, 6H, C₆H₅(DPPE)), 8.07(m, 4H, C₆H₅(DPPE)). ¹³C NMR (Acetone-*d*₆): 27.59(-CH₂-, DPPE), 82.57(η⁵-C₅H₅), 105.46(C₂), 118.63(C₇), 121.18(CN), 125.68(C₄), 125.92(C₆), 126.84(C₁₁), 128.01(C₁₀), 128.76(C₉), 129.05(CH, DPPE), 131.08(CH, DPPE), 133.26(CH, DPPE), 137.62(Cq, DPPE), 139.47(C₃), 140.93(C₈), 150.50(C₅). ³¹P NMR (Acetone-*d*₆): 79.1(s, DPPE). Anal. Found: C, 55.21; H, 3.82;

N, 1.51%. Calc. for $C_{43}H_{36}NS_3P_2F_3O_3Ru$: C, 55.48; H, 3.90; N, 1.50(%)

4.3.1.3. $[Fe(\eta^5-C_5H_5)(DPPE)(NC(C_4H_2S)C(H)C(H)(C_4H_3S))][PF_6]$ (**1Fe**). Orange-red; recrystallized from $CH_2Cl_2/(n\text{-hexane})$; 90% yield; IR (KBr, cm^{-1}): $\nu(CN)$ 2197, $\nu(PF_6^-)$ 839; 1H NMR (Acetone- d_6): 2.66(m, 2H, $-CH_2-$), 2.80(m, 2H, $-CH_2-$), 4.67(s, 5H, $\eta^5-C_5H_5$), 6.72(d, 1H, H_3 , $^3J_{HH} = 4.0$ Hz), 7.04(d, 1H, H_4 , $^3J_{HH} = 4.0$ Hz), 7.04(d, 1H, H_7 , $^3J_{HH} = 16.0$ Hz), 7.27(d, 1H, H_9 , $^3J_{HH} = 3.6$ Hz), 7.48(d, 1H, H_{11} , $^3J_{HH} = 5.1$ Hz), 7.56(m, 10H, $C_6H_5(DPPE)$), 7.64(m, 6H, $C_6H_5(DPPE)$), 8.07(m, 4H, $C_6H_5(DPPE)$). ^{13}C NMR (Acetone- d_6): 28.47($-CH_2-$, DPPE), 81.05($\eta^5-C_5H_5$), 107.18(C_2), 119.81(C_7), 126.53(C_4), 126.56(C_6), 127.63(C_{11}), 128.89(CN), 129.03(C_{10}), 129.58(C_9), 130.12(CH, DPPE), 132.44(CH, DPPE), 133.91(CH, DPPE), 137.63(Cq, DPPE), 140.18(C_3), 141.89(C_8), 150.62(C_5). ^{31}P NMR (Acetone- d_6): -144.1 (qt, $^1J_{P,F} = 710.2$ Hz, PF_6^-) 97.0(s, DPPE). Anal. Found: C, 55.55; H, 4.18; N, 1.55%. Calc. for $C_{42}H_{36}NS_2P_3F_6Fe \cdot 0.5CH_2Cl_2$: C, 55.24; H, 4.04; N, 1.52(%)

4.3.1.4. $[Ru(\eta^5-C_5H_5)(TMEDA)(NC(C_4H_2S)C(H)C(H)(C_4H_3S))][PF_6]$ (**2Ru**). Dark-orange; recrystallized from $CH_2Cl_2/(n\text{-hexane})$; 50% yield; IR (KBr, cm^{-1}): $\nu(CN)$ 2193, $\nu(PF_6^-)$ 839; 1H NMR (Acetone- d_6): 2.58(m, 4H, $-CH_2-$), 2.90(s, 6H, $-NCH_3$), 3.35(s, 6H, $-NCH_3$), 4.32(s, 5H, $\eta^5-C_5H_5$), 7.11(m, 1H, H_{10}), 7.24(d, 1H, H_7 , $^3J_{HH} = 16.0$ Hz), 7.31(d, 1H, H_9 , $^3J_{HH} = 3.4$ Hz), 7.38(d, 1H, H_4 , $^3J_{HH} = 3.6$ Hz), 7.47(d, 1H, H_6 , $^3J_{HH} = 16.0$ Hz), 7.52(d, 1H, H_{11} , $^3J_{HH} = 5.0$ Hz), 7.93(br, 1H, H_3). ^{13}C NMR (Acetone- d_6): 54.73(NCH_3 , TMEDA), 58.77(NCH_3 , TMEDA), 62.74($-CH_2-$, TMEDA), 70.38($\eta^5-C_5H_5$), 107.16(C_2), 118.45(CN), 119.99(C_7), 126.82(C_6), 127.31(C_4), 127.67(C_{11}), 129.05(C_{10}), 129.59(C_9), 140.81(C_8), 141.98(C_3), 151.67(C_5). ^{31}P NMR (Acetone- d_6): -144.2 (qt, $^1J_{P,F} = 711.2$ Hz, PF_6^-). Anal. Found: C, 38.66; H, 4.14; N, 6.01%. Calc. for $C_{22}H_{28}N_3S_2PF_6Ru \cdot 0.6CH_2Cl_2$: C, 39.02; H, 4.23; N, 6.04(%)

4.3.1.5. $[Ru(\eta^5-C_5H_5)(PPh_3)_2(NC(C_4H_2S)C(H)C(H)(C_4H_3S))][PF_6]$ (**3Ru**). Yellow; recrystallized from $CH_2Cl_2/(n\text{-hexane})$; 70% yield; IR (KBr, cm^{-1}): $\nu(CN)$ 2214, $\nu(PF_6^-)$ 840; 1H NMR (Acetone- d_6): 4.76(s, 5H, $\eta^5-C_5H_5$), 7.11(m, 1H, H_{10}), 7.20(d, 1H, H_7 , $^3J_{HH} = 15.9$ Hz), 7.24(m, 12H, $C_6H_5(PPh_3)$), 7.31(d, 1H, H_9 , $^3J_{HH} = 3.7$ Hz), 7.38(m, 14H, $C_6H_5(PPh_3)$), 7.47(m, 7H, $C_6H_5(PPh_3)$), 7.52(d, 1H, H_3 , $^3J_{HH} = 4.0$ Hz), (H_4 , H_6 , H_{11} under the phosphines). ^{13}C NMR (Acetone- d_6): 82.27($\eta^5-C_5H_5$), 105.35(C_2), 119.80(C_7), 126.18(CN), 127.07(C_6), 127.21(C_4), 127.85(C_{11}), 129.08(C_{10}), 129.42(CH, PPh_3), 129.78(C_9), 131.13(CH, PPh_3), 134.26(CH, PPh_3), 136.51(Cq, PPh_3), 141.32(C_3), 141.89(C_8), 151.98(C_5). ^{31}P NMR (Acetone- d_6): -144.1 (ht, $^1J_{P,F} = 712.6$ Hz, PF_6^-), 41.4(s, PPh_3). Anal. Found: C, 58.98; H, 4.37; N, 1.26%. Calc. for $C_{52}H_{42}NS_2P_3F_6Ru$: C, 59.31; H, 4.02; N, 1.33(%)

4.3.1.6. $[Ru(\eta^5-C_5H_5)(DPPE)(NC(C_4H_2S)C(H)C(H)(C_4H_2S)NO_2)][PF_6]$ (**4Ru**). Yellow; recrystallized from $CH_2Cl_2/(n\text{-hexane})$; 77% yield; IR (KBr, cm^{-1}): $\nu(CN)$ 2214, $\nu_{as}(OSO, CF_3SO_3^-)$ 1243; 1H NMR (Acetone- d_6): 2.69(m, 2H, $-CH_2-$), 2.80(m, 2H, $-CH_2-$), 5.03(s, 5H, $\eta^5-C_5H_5$), 6.82(d, 1H, H_3 , $^3J_{HH} = 4.0$ Hz), 7.24(d, 1H, H_4 , $^3J_{HH} = 4.0$ Hz), 7.32(d, 1H, H_6 , $^3J_{HH} = 16.0$ Hz), 7.36(d, 1H, H_9 , $^3J_{HH} = 4.4$ Hz), 7.48(d, 1H, H_7 , $^3J_{HH} = 16.0$ Hz), 7.52(m, 10H, $C_6H_5(DPPE)$), 7.63(m, 6H, $C_6H_5(DPPE)$), 7.99(d, 1H, H_{10} , $^3J_{HH} = 4.3$ Hz), 8.01(m, 4H, $C_6H_5(DPPE)$). ^{13}C NMR (Acetone- d_6): 27.64($-CH_2-$, DPPE), 82.69($\eta^5-C_5H_5$), 107.70(C_2), 120.68(CN), 123.91(C_6), 124.15(C_7), 127.32(C_9), 127.85(C_4), 128.98(CH, DPPE), 130.40(C_{10}), 131.07(CH, DPPE), 133.30(CH, DPPE), 137.33(Cq, DPPE), 139.68(C_3), 148.24(C_5), 148.59(C_8), 148.76(C_{11}). ^{31}P NMR (Acetone- d_6): 79.0(s, DPPE). Anal. Found: C, 51.71; H, 3.75; N, 2.96%. Calc. for $C_{42}H_{35}N_2S_2O_2P_3F_6Ru$: C, 51.11; H, 3.63; N, 2.88(%)

4.3.1.7. $[Ru(\eta^5-C_5H_5)(DPPE)(NC(C_4H_2S)C(H)C(H)(C_4H_2S)NO_2)][CF_3SO_3]$ (**4Ru**). Yellow; recrystallized from $CH_2Cl_2/(n\text{-hexane})$; 77% yield; IR (KBr, cm^{-1}): $\nu(CN)$ 2214, $\nu_{as}(OSO, CF_3SO_3^-)$ 1243; 1H NMR (Acetone- d_6): 2.70(m, 2H, $-CH_2-$), 2.80(m, 2H, $-CH_2-$), 5.02(s, 5H, $\eta^5-C_5H_5$), 6.82(d, 1H, H_3 , $^3J_{HH} = 4.0$ Hz), 7.20(d, 1H, H_4 , $^3J_{HH} = 4.0$ Hz), 7.33(d, 1H, H_6 , $^3J_{HH} = 16.0$ Hz), 7.36(d, 1H, H_9 , $^3J_{HH} = 4.4$ Hz), 7.47(d, 1H, H_7 , $^3J_{HH} = 16.0$ Hz), 7.50(m, 10H, $C_6H_5(DPPE)$), 7.63(m, 6H, $C_6H_5(DPPE)$), 8.00(d, 1H, H_{10} , $^3J_{HH} = 4.3$ Hz), 8.03(m, 4H, $C_6H_5(DPPE)$). ^{13}C NMR (Acetone- d_6): 27.64($-CH_2-$, DPPE), 82.69($\eta^5-C_5H_5$), 107.70(C_2), 120.68(CN), 123.91(C_6), 124.15(C_7), 127.32(C_9), 127.85(C_4), 128.98(CH, DPPE), 130.40(C_{10}), 131.07(CH, DPPE), 133.30(CH, DPPE), 137.33(Cq, DPPE), 139.68(C_3), 148.24(C_5), 148.59(C_8), 148.76(C_{11}). ^{31}P NMR (Acetone- d_6): 79.0(s, DPPE). Anal. Found: C, 52.85; H, 3.84; N, 2.80%. Calc. for $C_{43}H_{35}N_2S_3O_2P_3F_3Ru$: C, 52.97; H, 3.61; N, 2.87(%)

4.3.1.8. $[Fe(\eta^5-C_5H_5)(DPPE)(NC(C_4H_2S)C(H)C(H)(C_4H_2S)NO_2)][PF_6]$ (**4Fe**). Orange-red; recrystallized from $CH_2Cl_2/(n\text{-hexane})$; 93% yield; IR (KBr, cm^{-1}): $\nu(CN)$ 2193, $\nu(PF_6^-)$ 839; 1H NMR (Acetone- d_6): 2.67(m, 2H, $-CH_2-$), 2.84(m, 2H, $-CH_2-$), 4.70(s, 5H, $\eta^5-C_5H_5$), 6.79(d, 1H, H_3 , $^3J_{HH} = 4.0$ Hz), 7.21(d, 1H, H_4 , $^3J_{HH} = 4.0$ Hz), 7.29(d, 1H, H_6 , $^3J_{HH} = 16.0$ Hz), 7.36(d, 1H, H_9 , $^3J_{HH} = 4.3$ Hz), 7.46(d, 1H, H_7 , $^3J_{HH} = 16.0$ Hz), 7.56(m, 10H, $C_6H_5(DPPE)$), 7.65(m, 6H, $C_6H_5(DPPE)$), 7.99(d, 1H, H_{10} , $^3J_{HH} = 4.3$ Hz), 8.08(m, 4H, $C_6H_5(DPPE)$). ^{13}C NMR (Acetone- d_6): 27.58($-CH_2-$, DPPE), 80.33($\eta^5-C_5H_5$), 108.47(C_2), 123.61(C_6), 124.23(C_7), 127.23(C_9), 127.39(CN), 127.84(C_4), 129.22(CH, DPPE), 130.10(C_{10}), 131.52(CH, DPPE), 133.00(CH, DPPE), 136.64(Cq, DPPE), 139.25(C_3), 147.68(C_5), 148.33(C_8), 150.08(C_{11}). ^{31}P NMR (Acetone- d_6): -144.1 (qt, $^1J_{P,F} = 710.7$ Hz, PF_6^-), 97.0(s, DPPE). Anal. Found: C, 54.74; H, 3.83; N, 2.95%. Calc. for $C_{42}H_{35}N_2S_2O_2P_3F_6Fe$: C, 54.44; H, 3.81; N, 3.02(%)

4.3.1.9. $[Ru(\eta^5-C_5H_5)(TMEDA)(NC(C_4H_2S)C(H)C(H)(C_4H_2S)NO_2)][PF_6]$ (**5Ru**). Dark-orange; recrystallized from $CH_2Cl_2/(n\text{-hexane})$; 50% yield; IR (KBr, cm^{-1}): $\nu(CN)$ 2189, $\nu(PF_6^-)$ 839; 1H NMR (Acetone- d_6): 2.84(m, 4H, $-CH_2-$), 2.90(s, 6H, $-NCH_3$), 3.34(s, 6H, $-NCH_3$), 4.34(s, 5H, $\eta^5-C_5H_5$), 7.40(d, 1H, H_9 , $^3J_{HH} = 4.3$ Hz), 7.50(d, 1H, H_6 , $^3J_{HH} = 16.2$ Hz), 7.53(d, 1H, H_4 , $^3J_{HH} = 4.0$ Hz), 7.64(d, 1H, H_7 , $^3J_{HH} = 16.0$ Hz), 7.99(br, 1H, H_3), 8.01(d, 1H, H_{10} , $^3J_{HH} = 4.3$ Hz). ^{13}C NMR (Acetone- d_6): 54.77(NCH_3 , TMEDA), 58.81(NCH_3 , TMEDA), 62.77($-CH_2-$, TMEDA), 70.70($\eta^5-C_5H_5$), 109.52(C_2), 121.55(CN), 124.77(C_6), 125.34(C_7), 128.16(C_9), 129.51(C_4), 131.04(C_{10}), 140.96(C_3), 149.34(C_5), 149.63(C_8), 151.64(C_{11}). ^{31}P NMR (Acetone- d_6): -144.1 (ht, $^1J_{P,F} = 711.0$ Hz, PF_6^-). Anal. Found: C, 40.24; H, 4.13; N, 8.25%. Calc. for $C_{22}H_{27}N_4S_2O_2PF_6Ru \cdot 0.3C_6H_{14}$: C, 39.95; H, 4.40; N, 7.83(%)

4.3.1.10. $[Ru(\eta^5-C_5H_5)(PPh_3)_2(NC(C_4H_2S)C(H)C(H)(C_4H_2S)NO_2)][PF_6]$ (**6Ru**). Yellow; recrystallized from $CH_2Cl_2/(n\text{-hexane})$; 72% yield; IR (KBr, cm^{-1}): $\nu(CN)$ 2211, $\nu(PF_6^-)$ 840; 1H NMR (Acetone- d_6): 4.77(s, 5H, $\eta^5-C_5H_5$), 7.24(m, 12H, $C_6H_5(PPh_3)$), 7.38(m, 14H, $C_6H_5(PPh_3)$), 7.47(m, 6H, $C_6H_5(PPh_3)$), 7.58(d, 2H, $H_9 + H_3$, $J = 4.0$ Hz), 7.60(d, 1H, H_7 , $J = 16.1$ Hz), 8.00(d, 1H, H_{10} , $J = 4.0$ Hz), (H_4 , H_6 under the phosphines). ^{13}C NMR (Acetone- d_6): 84.49($\eta^5-C_5H_5$), 108.05(C_2), 124.22(C_6), 124.28(C_7), 125.01(CN), 127.42(C_9), 128.34(C_4), 128.54(CH, PPh_3), 130.13(C_{10}), 130.25(CH, PPh_3), 133.36(CH, PPh_3), 135.54(Cq, DPPE), 140.45(C_3), 148.28(C_5), 149.15(C_8), 150.25(C_{11}). ^{31}P NMR (Acetone- d_6): -144.0 (m, PF_6^-), 41.4(s, PPh_3). Anal. Found: C, 55.36; H, 3.95; N, 2.51%. Calc. for $C_{52}H_{41}N_2S_2O_2P_3F_6Ru \cdot 0.5CH_2Cl_2$: C, 55.29; H, 3.71; N, 2.46(%)

4.4. Electrochemical studies

The electrochemical experiments were performed on an EG&G Princeton Applied Research Model 273A potentiostat/galvanostat and monitored with a personal computer loaded with Electro-

chemistry PowerSuite v2.51 software from Princeton Applied Research. Cyclic voltammograms were obtained in 0.1 M solutions of $[\text{NBu}_4][\text{PF}_6]$ in dried CH_2Cl_2 or CH_3CN , at a three-electrode configuration cell, with a platinum-disk working electrode (1.0 mm diameter) probed by a Luggin capillary connected to a silver-wire pseudo-reference electrode; a Pt wire auxiliary electrode was employed. The electrochemical experiments were performed under a N_2 atmosphere at room temperature. The redox potentials of the complexes were measured at the presence of ferrocene, as the internal standard, and the redox potential values were normally quoted relative to the SCE by using the ferrocenium/ferrocene redox couple ($E_{\text{p}/2} = 0.46$ or 0.40 V versus SCE for CH_2Cl_2 or CH_3CN , respectively) [41].

4.5. X-ray crystallography

Pertinent details of data collection, structure solution and refinement parameters for the individual compounds can be found in Table 8. Crystallographic data for compounds **1Ru** and **4Ru** were collected using graphite monochromated Mo $K\alpha$ ($\lambda = 0.71069$ Å) radiation with a Bruker AXS-KAPPA APEX II area detector diffractometer equipped with an Oxford Cryosystem open-flow nitrogen cryostat; data were collected at 150 K for both compounds.

Cell parameters were retrieved using the Bruker SMART software and refined using SAINT [42] with all observed reflections. Absorption corrections were applied using SADABS [43].

Data for compound **1Fe** were collected at room temperature with a MACH3-Bruker Nonius diffractometer equipped with an Mo $K\alpha$ radiation ($\lambda = 0.71073$ Å) source. Data were corrected for Lorentz polarisation and for absorption effects by semiempirical methods based on ω -scans [44]. Data reduction was done with XCAD4 [45]. Cell dimensions were determined from the setting angles of 25 reflections, within θ values of 6.9° – 10.0° . All the structures were solved by direct methods using either SIR-97 [46] or SIR-2004 [47] and refined using full matrix least-squares refinement against F^2 , using SHELXL-97 [48]. All programs are included in the package of programs WINGX, version 1.64.05 [49]. All non-hydrogen atoms were refined anisotropically. The hydrogen atoms were inserted in idealised positions and allowed to refine as riding on the parent carbon atom except the acetylenic hydrogens between the thiophene rings in the ligand in compounds **1Ru** and **4Ru** and for the all the hydrogen atoms in the polythiophene ligand in compound **1Fe**. The molecular structures graphics were produced with ORTEP3 for Windows [50], included in the software package, and MERCURY [51].

In compound **4Ru** a severely disordered solvent molecule was found that could not be modelled so it was removed using SQUEEZE [52]. SQUEEZE calculated an electron count/cell of 104 which matches well with an *n*-hexane or dichloromethane molecule per asymmetric unit. Before SQUEEZE: $R_1 = 0.0900$; afterwards: $R_1 = 0.0764$.

In compound **1Fe** due to this data set being weak, with a drop off in intensity at moderate to higher angles, SHELL 8.0.83 was used to limit reflections for refinement. Due to severe anisotropy, restraints to anisotropic parameters (ISOR) were applied to all atoms in the refinement. One of the phenyl groups of the DPPE ligand (C121–C126) is also disordered over two sites but the disorder could not be modelled.

Acknowledgements

The authors thank to Fundação Para a Ciência e Tecnologia (FCT) for financial support (POCTI/QUI/48443/2002). Pedro Florindo thanks FCT for the Ph.D. grant conceded (SFRH/BD/12432/2003).

Appendix A. Supplementary material

CCDC 694644–694646 contain the supplementary crystallographic data for compounds **1Ru**, **4Ru** and **1Fe**. These data can be obtained free of charge from The Cambridge Crystallographic Data Centre via www.ccdc.cam.ac.uk/data_request/cif. Supplementary data associated with this article can be found, in the online version, at doi:10.1016/j.jorganchem.2008.11.019.

References

- [1] M.L.H. Green, S.R. Marder, M.E. Thompson, J.A. Bandy, D. Bloor, P.V. Kolinsky, R.J. Jones, *Nature* 330 (1987) 360.
- [2] H.S. Nalwa, *Appl. Organomet. Chem.* 5 (1991) 349.
- [3] N.J. Long, *Angew. Chem., Int. Ed. Engl.* 34 (1995) 21.
- [4] S.R. Marder, in: D.W. Bruce, D. O'Hare (Eds.), *Inorganic Materials*, second ed., Wiley, Chichester, 1996, p. 121.
- [5] T. Verbiest, S. Houbrechts, M. Kauranen, K. Clays, A. Persoons, *J. Mater. Chem.* 7 (1997) 2175.
- [6] H. Le Bozec, T. Renouard, *Eur. J. Inorg. Chem.* (2000) 229.
- [7] E. Goovaerts, W.E. Wenseleers, M.H. Garcia, G.H. Cross, in: H.S. Nalwa (Ed.), *Handbook of Advanced Electronic and Photonic Materials*, vol. 9, Academic Press, 2001, p. 127 (Chapter 3).
- [8] S. Di Bella, *Chem. Soc. Rev.* 30 (2001) 355.
- [9] (a) I.R. Whittall, A.M. McDonagh, M.G. Humphrey, M. Samoc, *Adv. Organomet. Chem.* 42 (1998) 291; (b) J.P. Morral, G.T. Dalton, M.G. Humphrey, M. Samoc, *Adv. Organomet. Chem.* 55 (2008) 61.
- [10] For a review on metallocenes for NLO purposes: S. Barlow, S.R. Marder, *Chem. Commun.* (2000) 1555.
- [11] W. Wenseleers, A.W. Gerbrandij, E. Goovaerts, M.H. Garcia, M.P. Robalo, P.J. Mendes, J.C. Rodrigues, A.R. Dias, *J. Mater. Chem.* 8 (1998) 925.
- [12] M.H. Garcia, M.P. Robalo, A.R. Dias, M.F.M. Piedade, A. Galvão, M.T. Duarte, W. Wenseleers, E. Goovaerts, *J. Organomet. Chem.* 619 (2001) 252.
- [13] M.H. Garcia, M.P. Robalo, A.R. Dias, M.T. Duarte, W. Wenseleers, G. Aerts, E. Goovaerts, M.P. Cifuentes, S. Hurst, M.G. Humphrey, M. Samoc, B. Luther-Davies, *Organometallics* 21 (2002) 2107.
- [14] C.E. Powell, M.G. Humphrey, *Coord. Chem. Rev.* 248 (2004) 725.
- [15] M.P. Cifuentes, M.G. Humphrey, *J. Organomet. Chem.* 689 (2004) 3968.
- [16] A.K. Jen, V.P. Rao, K.Y. Wong, K.J. Drost, *J. Chem. Soc., Chem. Commun.* (1993) 90.
- [17] M. Szablewski, P.R. Thomas, A. Thornton, D. Bloor, G.H. Cross, J.M. Cole, J.A.K. Howard, M. Malagoli, F. Meyers, J.-L. Brédas, W. Wenseleers, E. Goovaerts, *J. Am. Chem. Soc.* 119 (1997) 3144.
- [18] T.J.J. Müller, J.P. Robert, E. Schmäzlin, C. Bräuchle, K. Meerholz, *Org. Lett.* 2 (2000) 2419.
- [19] R.D.A. Hudson, A.R. Manning, D.F. Nolan, I. Asselberghs, R. Van Boxel, A. Persoons, J.F. Gallagher, *J. Organomet. Chem.* 619 (2001) 141.
- [20] R.D.A. Hudson, I. Asselberghs, K. Clays, L.P. Cuffe, J.F. Gallagher, A.R. Manning, A. Persoons, K. Wostyn, *J. Organomet. Chem.* 435 (2001) 637.
- [21] M.H. Garcia, S. Royer, M.P. Robalo, A.R. Dias, J.-P. Tranchier, R. Chavignon, D. Prim, A. Auffrant, F. Rose-Munch, E. Rose, J. Vaissermann, A. Persoons, I. Asselberghs, *Eur. J. Inorg. Chem.* (2003) 3895.
- [22] B. Insuasty, C. Atienza, C. Seoane, N. Martín, J. Gann, J. Orduna, R. Alcalá, B. Villacampa, *J. Org. Chem.* 69 (2004) 6986.
- [23] J.-L. Fillaut, J. Perruchon, P. Blanchard, J. Roncali, S. Golhen, M. Allain, A. Migalsaka-Zalas, I.V. Kityk, B. Sahraoui, *Organometallics* 24 (2005) 687.
- [24] Y. Liao, B.E. Eichinger, K.A. Firestone, M. Haller, J. Luo, W. Kaminsky, J.B. Benedict, P.J. Reid, A.K.-Y. Jen, L.R. Dalton, B.H. Robinson, *J. Am. Chem. Soc.* 127 (2005) 2758.
- [25] A.-L. Roy, M. Chavarot, É. Rose, F. Rose-Munch, A.-J. Attias, D. Kréher, J.-L. Fave, C. Kamierszky, *CR Chim.* 8 (2005) 1256.
- [26] M.H. Garcia, P.J. Mendes, M.P. Robalo, A.R. Dias, J. Campo, W. Wenseleers, E. Goovaerts, *J. Organomet. Chem.* 692 (2007) 3027.
- [27] M. Ciofalo, G. La Manna, *Chem. Phys. Lett.* 263 (1996) 73.
- [28] T.L. Porter, D. Minore, D. Zhang, *J. Phys. Chem.* 99 (1995) 13213.
- [29] M. Ephritikhine, *Chem. Commun.* 23 (1998) 2549.
- [30] A.R. Dias, M.H. Garcia, J.C. Rodrigues, M.L.H. Green, K.K. Lai, S.M. Klueber, *J. Organomet. Chem.* 475 (1994) 241.
- [31] M.H. Garcia, P. Florindo, M.F.M. Piedade, M.T. Duarte, M.P. Robalo, J. Heck, C. Wittenburg, J. Holtmann, E. Licandro, *J. Organomet. Chem.* 693 (2008) 2987.
- [32] J. Roncali, P. Marque, R. Garreau, F. Garnier, M. Lemaire, *Macromolecules* 23 (1990) 1347.
- [33] P. Mendes, Ph.D. Thesis, University of Lisbon, Faculty of Sciences, 2001.
- [34] J. Rodrigues, Ph.D. Thesis, University of Lisbon, Faculty of Sciences, 1999.
- [35] R.L. Cordiner, D. Albesa-Jové, R.L. Roberts, J.D. Farmer, H. Puschmann, D. Corcoran, A.E. Goeta, J.A.K. Howard, P.J. Low, *J. Organomet. Chem.* 690 (2005) 4908.
- [36] M.T. Duarte, M.F.M. Piedade, M.P. Robalo, C. Jacob, M.H. Garcia, *Acta Crystallogr. C62* (2006) m531.
- [37] W. Wenseleers, E. Goovaerts, P. Hepp, M.H. Garcia, M.P. Robalo, A.R. Dias, M.F.M. Piedade, M.T. Duarte, *Chem. Phys. Lett.* 367 (2003) 390.

- [38] D.D. Perrin, W.L.F. Amarego, D.R. Perrin, *Purification of Laboratory Chemicals*, second ed., Springer, Berlin, 1980.
- [39] G.S. Ashby, M.I. Bruce, I.B. Tomkins, R.C. Walli, *Aust. J. Chem.* 32 (1979) 1003.
- [40] Y. Ohki, N. Uehara, H. Suzuki, *Organometallics* 22 (2003) 59.
- [41] N.G. Connelly, W.E. Geiger, *Chem. Rev.* 96 (1996) 877.
- [42] SAINT: Area-Detector Integration Software (Version7.23), Bruker AXS Inc., Madison, WI, 2004.
- [43] sadabs: Area-Detector Absorption Correction, Bruker AXS Inc., Madison, WI, 2004.
- [44] A.C.T. North, D.C. Phillips, F.S. Mathews, *Acta Crystallogr. Sect. A* 24 (1968) 351.
- [45] K. Harms, S. Wocadlo, XCAD4-CAD4 Data Reduction, University of Marburg, Marburg, Germany, 1995.
- [46] A. Altomare, M.C. Burla, M. Camalli, G. Cascarano, G. Giacovazzo, A. Guagliardi, A.G.G. Moliterini, G. Polidoro, R. Spagna, *J. Appl. Crystallogr.* 32 (1999) 115.
- [47] M.C. Burla, M. Camalli, B. Carrozzini, G.L. Cascarano, C. Giacovazzo, G. Polidori, R. Spagna, *J. Appl. Crystallogr.* 36 (2003) 1103.
- [48] G.M. Sheldrick, *SHELXL-97: Program for the Refinement of Crystal Structure*, University of Gottingen, Germany, 1997.
- [49] L.J. Farrugia, *J. Appl. Crystallogr.* 32 (1999) 837.
- [50] L.J. Farrugia, *J. Appl. Crystallogr.* 30 (1997) 565.
- [51] C.F. Macrae, P.R. Edgington, P. McCabe, E. Pidcock, G.P. Shields, R. Taylor, M. Towler, J. Van der Streek, *J. Appl. Crystallogr.* 39 (2006) 453.
- [52] P. Van der Sluis, A.L. Spek, *Acta Crystallogr. Sect. A* 46 (1990) 194.